



Consortium Members



National
Oceanography Centre
NATURAL ENVIRONMENT RESEARCH COUNCIL



CCI_Sea_Level_Bridging_Phase Characterisation of altimetry errors and uncertainties

Characterisation of altimetry errors and uncertainties



Chronology Issues:			
Issue:	Date:	Reason for change:	Author
1.0	16/01/2019	Creation	Michaël Ablain, Benoît Meysignac, Pierre Prandi
2.0	31/03/2019	Updated version	Pierre Prandi
2.1	01/07/2019	Response to reviews	Pierre Prandi

People involved in this issue:		
Written by (*):	Pierre Prandi	Date + Initials:(visa or ref)
Checked by (*):	JF Legeais	Date + Initial:(visa ou ref)
Approved by (*):	JF Legeais	Date + Initial:(visa ou ref)
Application authorized by (*):	J. Benveniste	Date + Initial:(visa ou ref)

**In the opposite box: Last and First name of the person + company if different from CLS*

Index Sheet:	
Context:	SL_cci
Keywords:	Oceanography sea level
Hyperlink:	

Distribution:		
Company	Means of distribution	Names
CLS	Notification	



LIST OF ACRONYMS

CCI: Climate Change Initiative

CTOH: Centre de Topographie de l'Océan et de l'Hydrosphère

GMSL: Global Mean Sea Level

LEGOS: Laboratoire d'Etudes en Géophysique et Océanographie Spatiale

LRM: Low Resolution Mode

TUM Technical University Munich



Table of content

1. Introduction.....	5
2. Altimetry errors and sea level uncertainties at global scale	7
2.1. GMSL errors and uncertainties	7
2.1.1. Mathematical description	7
2.1.2. Altimeter errors.....	7
2.1.3. Resulting uncertainties.....	9
3. Uncertainties in coastal sea level trends	10
3.1. Data & Methods.....	10
3.2. Results & discussion	11
4. REFERENCES	14
5. Annex 1: Uncertainty in Satellite estimate of Global Mean Sea Level changes, trend and acceleration - draft version.....	16
1 Introduction.....	16
1 GMSL data series.....	18
2 Altimetry GMSL error budget	19
3 The GMSL error variance-covariance matrix.....	20
4 GMSL uncertainty envelope	21
5 Uncertainty in GMSL trend and acceleration.....	22
6 Conclusions	24
Data	24
Acknowledgment	25
References	25



1. Introduction

During the 1st phase (2011-2013) of the CCI sea level project, new, optimized algorithms have been selected for the production of a first set of sea level gridded time series (Ablain et al., 2017, Quartly et al., 2017). During phase II (2014-2016), the sea level time series produced during phase I have been extended and some algorithms have been improved. Therefore, a full reprocessing of monthly sea level gridded time series was carried out over 1993-2015 and this dataset is now freely available for the users (Legeais et al., 2018). This new product benefits from the development of improved radar altimeter standards, leading to better sea level data and reduced altimetry errors. The CCI sea level project has benefited from a 1-year extension (from March 2018 to March 2019), with two main objectives:

- Characterization of altimetry errors on the CCI sea level products at global and regional scales
- Production of new sea level datasets dedicated to coastal applications in a few selected coastal areas

In the context of these additional activities (called SL_cci_Bridging Phase (SL_cci_BP)), it was indeed proposed to investigate the rate of sea level change in selected coastal zones, combining the recent technical advances allowed by different efforts done in the coastal altimetry community. Retracked altimetry data from LRM missions provided by TUM (Passaro et al., 2018a, 2018b), obtained using the ALES retracker and geophysical corrections dedicated to coastal areas were combined using the X-TRACK processing algorithm developed at LEGOS/CTOH (Birol et al., 2017). In this 1-year project, focus was made in 3 pilot regions: western Africa, Mediterranean Sea and northeastern Europe (Fig.1). Two LRM missions have been considered: Jason-1 and Jason-2, over the period from July 2002 to June 2016 (eg 14 full years). Only along-track sea level products have been produced.

The present document focuses on the determination of uncertainties associated to sea level time

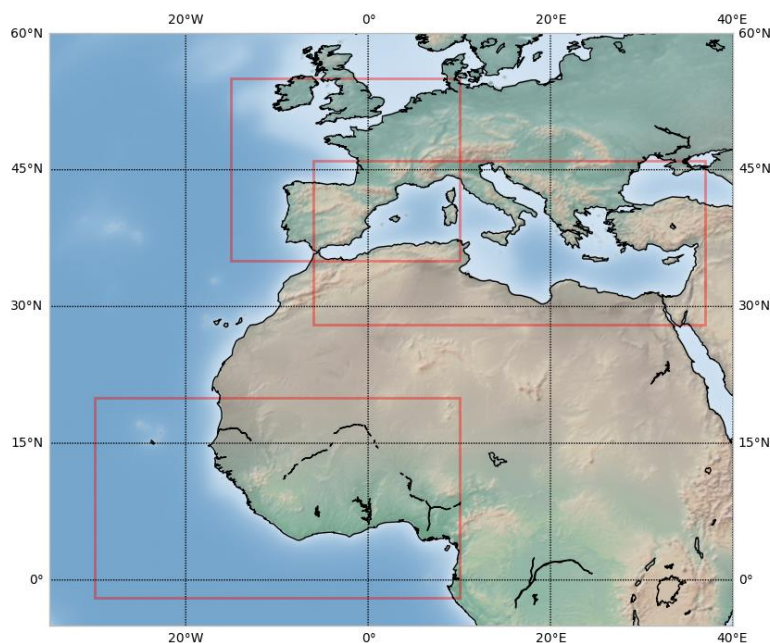


Figure 1, The three pilot regions considered for the CCI Sea Level 'Bridging Phase' project



series, both at the global and regional scales.

Two different approaches are considered to derive MSL uncertainties:

- For the GMSL, we estimate an *a priori* error description that covers the main contributions to the measurement system errors, and derive GMSL uncertainties from these errors. A brief description of the methodology and results is available in section 2, a more detailed analysis is available in the submitted paper (included as an Annex to this report, p. 16)
- For coastal trends, no comprehensive description of the error is available, and an ensemble approach is used to derive uncertainties, the method and its results are presented in section 3.



2. Altimetry errors and sea level uncertainties at global scale

Satellite altimetry now provides more than 25 years of measurement of the sea surface topography. These measurements are continuous and provide a quasi-global coverage of the ocean. Several groups use along-track measurements to compute global mean sea level averages which is an essential climate change indicator.

Estimating a reliable uncertainty and providing it to GMSL users is crucial for:

- the precise determination of the trend and acceleration of the GMSL record,
- the analysis of the sea level budget closure,
- understanding mechanisms driving sea level rise,
- detecting and attributing sea level changes to anthropogenic climate change.

The work performed in the scope of the SL-CCI Bridging Phase addresses this topic using two approaches. One focuses on the estimation of errors affecting the GMSL record in a budget approach where individual error contributions are combined and used to estimate uncertainties on the trend and acceleration of the GMSL record. The second uses a probabilistic ensemble-based approach to study the level of uncertainty of coastal sea level trends.

The investigations performed and their results are summarized below.

2.1. GMSL errors and uncertainties

The approach proposed here builds upon previous work (Ablain et al., 2009, 2015). The results are currently being submitted for publication, and a draft version of the manuscript is included in this report (see section 5). The work is summarized here, with highlights on new findings with respect to the Ablain et al., 2015 paper.

2.1.1. Mathematical description

Ablain et al., 2009 proposed, among other methods, to use an inverse formulation to estimate the confidence interval on the GMSL rise rate. At the time, they concluded that the uncertainty was +/- 0,6 mm/yr. This method requires an a priori knowledge on the error structure (expressed through the variance-covariance matrix) affecting the measurements.

For example, let $Y = X\beta + \varepsilon$, where β is the vector of a degree one polynomial function, then the ordinary least squares method provides an unbiased estimator of β : $\hat{\beta} = (X^t X)^{-1} X^t Y$. In general errors are supposed to be independent and identically distributed which leads to $\hat{\beta}$ following a normal law $N(\beta, \sigma)$ where σ is empirically determined from the distribution of the residuals to the fit. In a more general case where the error structure has a more complex variance-covariance matrix (Σ) then $\hat{\beta}$ remains an unbiased estimator but its distribution is modified and follows $N(\beta, (X^t X)^{-1} (X^t \Sigma X) (X^t X)^{-1})$.

The confidence interval is derived from this distribution at any given confidence level (here 90% corresponding to $1,65\sigma$).

2.1.2. Altimeter errors

As described in the previous paragraph, the uncertainty estimates relies heavily on the error variance-covariance matrix. The estimation of this matrix relies on a large knowledge based, mainly coming from Cal/Val activities performed on the different missions. Table 1 presents the different errors affecting satellite altimeter measurements which are applied in the present study. These errors fall into three categories: correlated errors, drifts and biases. Each category has an error covariance model, which is scaled to the amplitude of the error.



Source of errors	Error category	Uncertainty level (at 1 σ)	Reference
High frequency errors: altimeter noise, geophysical corrections, orbits ...	Correlated errors ($\lambda = 2$ months)	$\sigma = 1.7$ mm for TOPEX period $\sigma = 1.5$ mm for Jason-1 period. $\sigma = 1.2$ mm for Jason-2/3 period.	See Annex 1
Medium frequency errors: geophysical corrections, orbits ..	Correlated errors ($\lambda = 1$ year)	$\sigma = 1.3$ mm for TOPEX period $\sigma = 1.2$ mm for Jason-1 period. $\sigma = 1$ mm for Jason-2/3 period.	See Annex 1
Large frequency errors: wet troposphere correction	Correlated errors ($\lambda = 5$ years)	$\sigma = 1.1$ mm over all the period (\Leftrightarrow to 0.2 mm/yr for 5 years)	Legeais et al., 2014 Thao et al., 2014
Large frequency errors: orbits (Gravity fields)	Correlated errors ($\lambda = 10$ years)	$\sigma = 1.12$ mm over TOPEX period (no GRACE data) $\sigma = 0.5$ mm over Jason period (\Leftrightarrow to 0.05 mm/yr for 10 years)	Couhert et al., 2015 Rudenko et al., 2017
Altimeter instabilities on TOPEX-A and TOPEX-B	Drift error	$\delta = 0.7$ mm/yr on TOPEX-A period $\delta = 0.1$ mm/yr on TOPEX-B period	Ablain, 2017 Beckley et al., 2017 Watson et al., 2015
Long-term drift errors: orbit (ITRF) and GIA	Drift error	$\delta = 0.12$ mm/yr over 1993-2017	Couhert et al., 2015 Spada et al., 2017
GMSL bias errors to link altimetry missions together	Bias errors	$\Delta = 2$ mm for TP-A/TP-B $\Delta = 0.5$ mm for TP-B/J1, J1/J2, J2/J3.	Zawadzki et al., 2018

Table 1, GMSL error sources given at 1 sigma level

With respect to previous error estimations by Ablain et al. (2009, 2015) the error description used here is much more detailed, in particular efforts were made on :

- The heteroscedasticity of the error over the time series for time-correlated errors and drifts, this allows for a better description of the early drift of TOPEX-A for example,
- The description of long-period correlated errors to account for instabilities of the wet tropospheric correction. These used to be described as drifts and are now considered as long-period errors with decorrelation scales of 5 years,
- Addition of orbit errors due to the time varying gravity field with decorrelation scale of 10 years.

Individual error terms are considered to be independent and to total error variance-covariance matrix is obtained by summing up the individual error matrices. The total error variance-covariance matrix is displayed on Figure 2. This clearly shows higher error levels at the beginning of the period. Negative covariances between the early and latest parts of the record (for example between Jason-3 and TOPEX-A) result from orbit drifts errors that affect in opposite ways the time series ends.

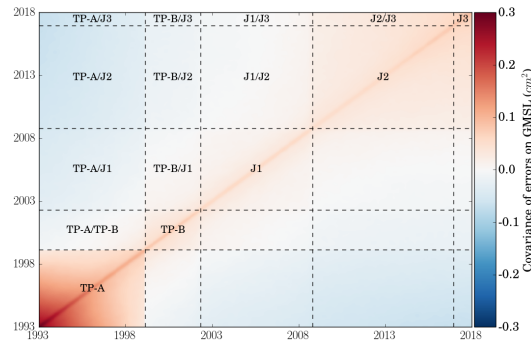


Figure 2, GMSL error variance-covariance matrix over 25 years

2.1.3. Resulting uncertainties

The variance-covariance matrix derived in the previous section can be used to estimate the uncertainty on the trend (and acceleration) of the GMSL record over any given time period. Results are summarized on Figure 3. The y-axis represents the length of the record from 2 to 25 years and the x-axis represents the central date of the sub-record used (so the first date is 1994 corresponding to the [1993,1995] period).

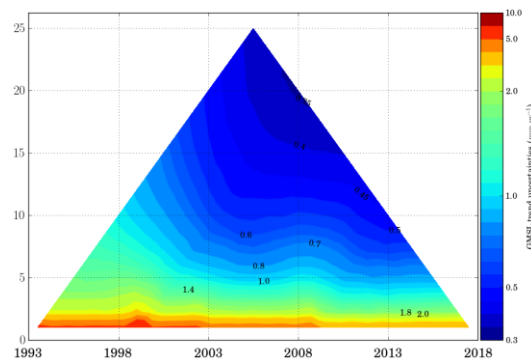


Figure 3, GMSL trend uncertainty in mm/yr at the 90% confidence level as a function of the time series length and time period.

Over the full record an uncertainty of +/- 0.4 mm/yr is estimated. Interestingly uncertainties down to +/- 0.35 mm/yr are reached over 20 years periods centered around 2008, which exclude the higher error TOPEX-A record.

A similar analysis was performed for the acceleration of the GMSL record, resulting in a +/- 0.07 mm/yr² acceleration uncertainty over the whole GMSL record. This result also means that significant sea level accelerations are observed (see Section 5, page 16).

The results presented here are based on the current knowledge of errors affecting satellite altimeter measurements. This error budget should be revised regularly to account for new findings. The budget presented here does not account for the internal variability of the system, only for errors affecting the measurement system.



3. Uncertainties in coastal sea level trends

During the SL-CCI Bridging Phase, a large effort has been devoted to the retrieval of sea surface topography measurements at the coast. Indeed a comprehensive knowledge of coastal sea level variability is of extreme importance for communities trying to adapt to sea level rises. While coastal sea level can be monitored by tide gauges, such instruments are scarce in large parts of the world, where altimetry can therefore provide valuable insights.

However there are several reasons that might impeded the capabilities of altimetry in coastal areas:

- Contamination of land in the waveform footprint,
- Contamination of land in the radiometer footprint,
- Unmodeled local tidal effects,
- Modification of the wave field properties with bathymetric features,
- ...

Strategies exist to mitigate these impacts, such as an improved retracking algorithm for example. Again estimating reliable uncertainties on coastal measurements is crucial for the detection of significant signals in coastal sea level.

3.1. Data & Methods

To perform this task, we adopt a different method from the one used in section 2.1 which is not applicable due to the lack of a description of the error variance-covariance structure near the coast. To overcome this limitation, we adopt an ensemble based approach: for each measurement along the mean profile we generate an ensemble of sea level time series using different combinations of standards and/or geophysical corrections. The uncertainty is then estimated from the spread of the ensemble.

The analysis is performed using data from TOPEX/Poseidon, Jason-1 and Jason-2 which share the same ground track. All tracks are projected on the theoretical ground track to produce a spatial sampling that does not change from one cycle to another (see Figure 4). We use a combination of an orthogonal projection and a spline interpolation to perform the reprojection on the position of theoretical measurements.

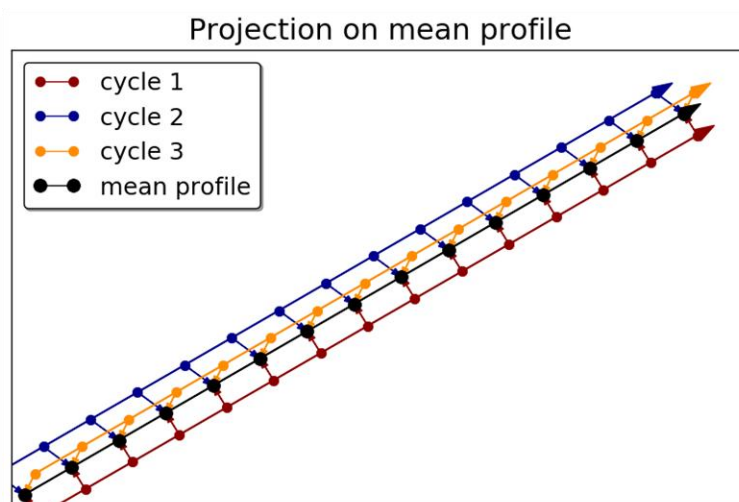


Figure 4, Example of the projection of along-track data on the theoretical ground track position

For each measurement of the theoretical ground track (black dots on Figure 4) time series are constructed by accumulating cycles. An ensemble of time series is generated by using different combinations of geophysical corrections to estimate the sea level. The different combinations used are summarized in Table 2. The corrections selected leave an ensemble of 320 members.



Correction	Number	Members
mean sea surface	2	CNESCLS15 (Schaeffer et al., 2016), DTU2015(Andersen et al., 2016)
ocean tide	2	GOT4V10 (Ray et al., 2013), FES2014 (Carrère et al., 2016)
Wet tropospheric correction	5	Radiometer, radiometer-alg01, ERA Interim, ECMWF, GPD+
DAC	2	ERA Interim, MOG2D
Dry tropospheric correction	2	ECMWF, ERA Interim
Ionospheric correction	2	ERA Interim, dual frequency correction
Editing	2	Coastal, open ocean

Table 2, List of the different members used to generate the ensemble of sea level time series

At each point along the theoretical ground track, the local sea level trend uncertainty is estimated from the standard deviation of the distribution of the trends of all members.

3.2. Results & discussion

The methodology described above was applied to three regions matching the ones used in the SL_cci_BP : the Mediterranean Sea, Western Europe and Western Africa. The standard deviation of sea level trends from the ensemble are displayed on Figure 5, Figure 6 and Figure 7. Bathymetry contours are displayed as thin black lines. All three maps show that uncertainties are higher at the coast, as expected. However, this rise in uncertainty does not seem to affect all coasts equally, and high standard deviation areas are sometimes observed in the open ocean (off the coast of Ireland for example), which would require further investigations.

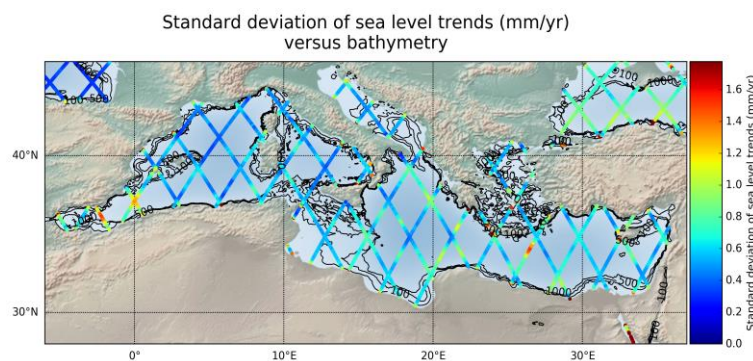


Figure 5, standard deviation of sea level trends (mm/yr) from an ensemble of 320 members in the Mediterranean Sea

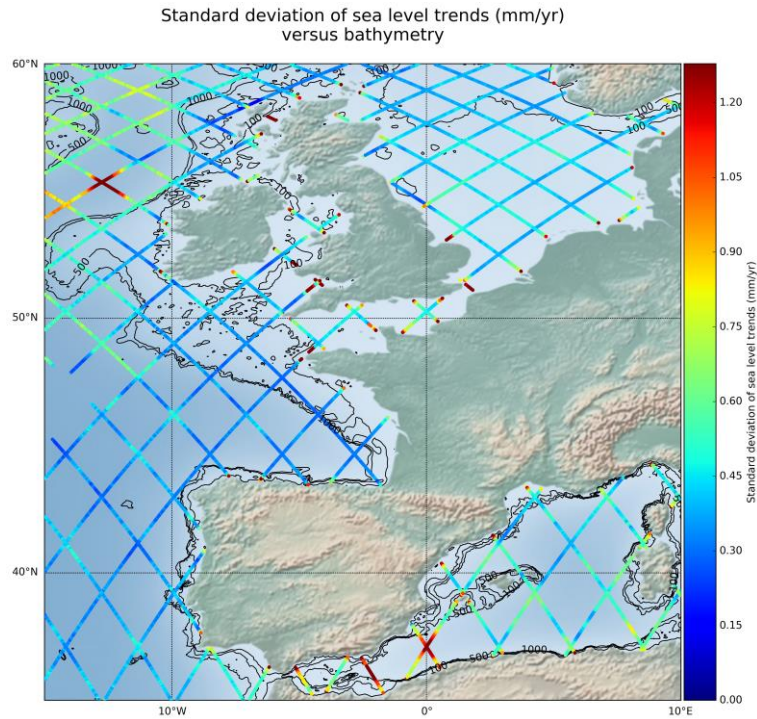


Figure 6, standard deviation of sea level trends (mm/yr) from an ensemble of 320 members in Western Europe

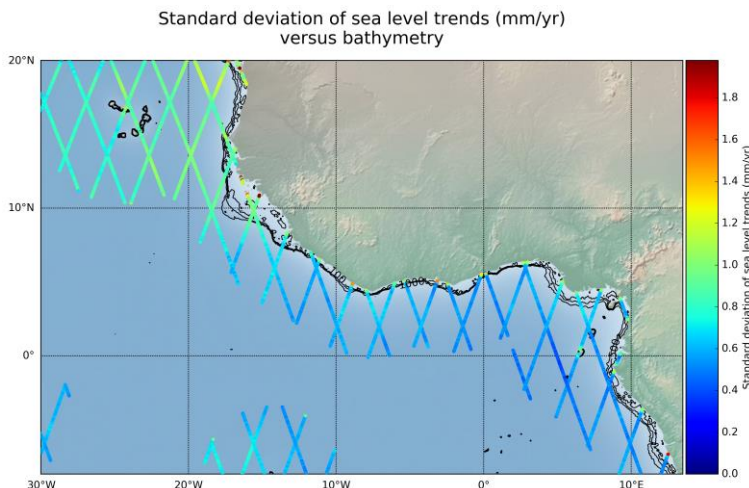


Figure 7, standard deviation of sea level trends (mm/yr) from an ensemble of 320 members in Western Africa

To assess the dependence between the trends and their standard deviation and the distance to the coast and/or bathymetry, all data points in the previous maps were binned along the distance to the nearest coast and bathymetry. For the trends themselves (see Figure 8) apart from the Mediterranean Sea area, we find no visible pattern that would indicate a greater sea level rise at the coast than in the neighbouring open ocean.

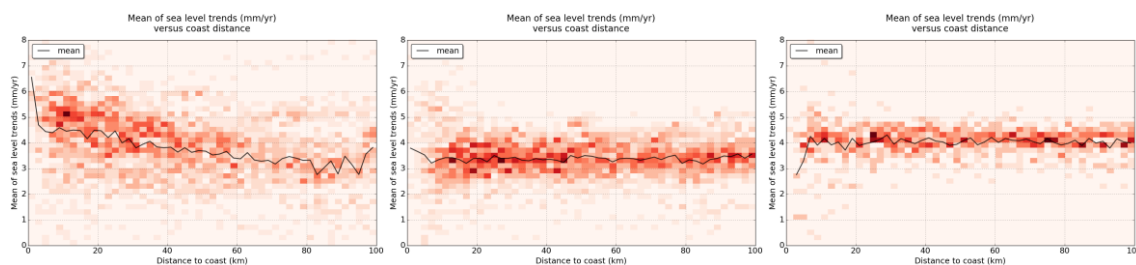


Figure 8, density of sea level trends (mm/yr) with respect to the distance to the nearest coast for the Mediterranean Sea (left), Western Europe (center) and Western Africa (right)

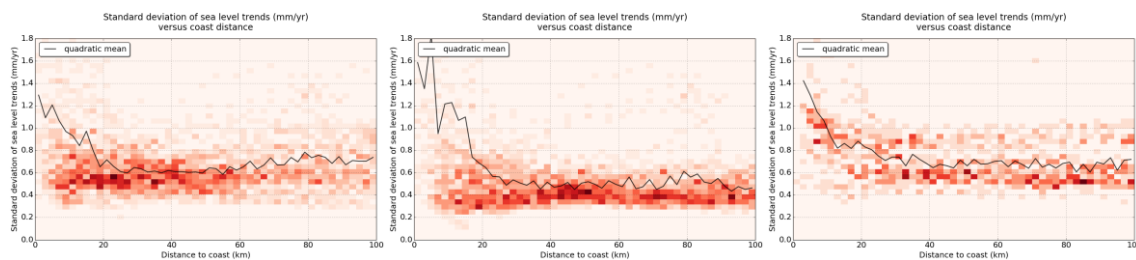


Figure 9, density of sea level trends standard deviation (mm/yr) with respect to the distance to the nearest coast for the Mediterranean Sea (left), Western Europe (center) and Western Africa (right)

Regarding the standard deviation of trends (Figure 9) all three regions show an important rise below 30 km from the coast. The standard deviation of sea level trends rises from 0,6 mm/yr to 1,2 mm/yr near the coast. The observation of the same behaviour in all regions considered suggests a robust pattern. Such rise in the uncertainty at the coast also suggests that rise in the trend itself observed in the Mediterranean Sea is likely not significant.

It is important to note however than these results are estimated from an open ocean oriented processing which uses the MLE4 retracking algorithm and 1Hz data only. There are likely some close coast features that are not observable in 1Hz data that could become observable on high rate data, as suggested by the other works performed within the SL_cci_BP project.



In addition to the previously described metrics, one can use the ensemble to affect the total error to one (or several) of the corrections that were used to generate members. The correction that explains the largest part of the uncertainty is called the predominant factor, and its contribution to the uncertainty is called its proeminence.

An example of predominant contributions maps is given in Figure 10, for the Mediterranean Sea. In all regions considered, the wet tropospheric correction is by far the largest contributor to the total uncertainty. The wet tropospheric correction explains about 80% of the observed trend variability. This remains true in all three regions considered in this study (Europe et Western Africa not shown).

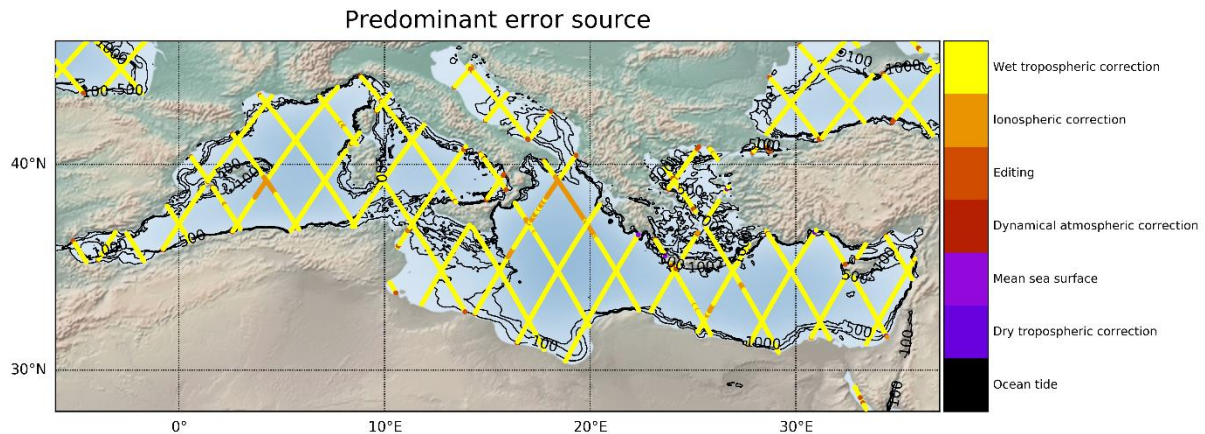


Figure 10, predominant error source in the Mediterranean Sea

It should be noted that the ensemble generation process uses 5 different solutions for wet tropospheric correction, as opposed to only two for other corrections. Therefore, it is not unexpected to find that the wet tropospheric correction as the main contributor to the ensemble spread, even if all wet tropospheric corrections selected are considered of equivalent quality. A leave-one-out validation could provide valuable insights on this matter.

Of course the coastal sea level trends uncertainties presented here do have limitations:

- They do not include the contribution of sea level's internal variability, as we only get to observe one realisation of this process,
- Their reliability is based on the assumption that the corrections selected to build the ensemble sample uniformly the range of plausible realisations, which is difficult to establish,
- Ideally, they should be revised regularly to include new corrections, and any new knowledge about radar altimeter measurements of sea level in the coastal zone.

4. REFERENCES

Ablain, M., Legeais, J.F., Prandi, P., Fenoglio-Marc L., Marcos M., Benveniste J., Cazenave A., 2017, Satellite Altimetry-Based Sea Level at Global and regional Scales, *Surv Geophys*, 38: 7. doi:10.1007/s10712-016-9389-8

Ablain, M., Cazenave, A., Larnicol, G., Balmaseda, M., Cipollini, P., Faugère, Y., Fernandes, M. J., Henry, O., Johannessen, J. A., Knudsen, P., Andersen, O., Legeais, J., Meyssignac, B., Picot, N., Roca, M., Rudenko, S., Scharffenberg, M. G., Stammer, D., Timms, G., and Benveniste, J.: Improved sea level record over the satellite altimetry era (1993-2010) from the Climate Change Initiative project, *Ocean Sci.*, 11, 67-82, <https://doi.org/10.5194/os-11-67-2015>, 2015.



Ablain, M., Cazenave, A., Valladeau, G., and Guinehut, S.: A new assessment of the error budget of global mean sea level rate estimated by satellite altimetry over 1993-2008, *Ocean Sci.*, 5, 193-201, <https://doi.org/10.5194/os-5-193-2009>, 2009.

Andersen, Ole Baltazar; Stenseng, Lars; Piccioni, Gaia; Knudsen, Per, The DTU15 MSS (Mean Sea Surface) and DTU15LAT (Lowest Astronomical Tide) reference surface, ESA Living Planet Symposium, 2016

Birol, F., Fuller, N., Lyard, F., Cancet, M., Niño, F., Delebecque, C., Fleury, S., Toubanc, F., Melet, A., Saraceno, M., Léger, F., 2017. Coastal applications from nadir altimetry: Example of the X-TRACK regional products. *Advances in Space Research* 59, 936-953. <https://doi.org/10.1016/j.asr.2016.11.005>

Carrère L., Lyard F., Cancet M., Guillot A., Picot N., 2016, FES 2014, a new tidal model: validation results and perspectives for improvements, in Proc. at ESA Living Planet Conf. , Prague, Czech Republic, European Space Agency.

Legeais, J.-F., Ablain, M., Zawadzki, L., Zuo, H., Johannessen, J. A., Scharffenberg, M. G., Fenoglio-Marc, L., Fernandes, M. J., Andersen, O. B., Rudenko, S., Cipollini, P., Quartly, G. D., Passaro, M., Cazenave, A., and Benveniste, J.: An improved and homogeneous altimeter sea level record from the ESA Climate Change Initiative, *Earth Syst. Sci. Data*, 10, 281-301, <https://doi.org/10.5194/essd-10-281-2018>, 2018.

Passaro, M., Z. A. Nadzir, G. D. Quartly, 2018a, Improving the precision of sea level data from satellite altimetry with high-frequency and regional sea state bias corrections, *Remote Sensing of the Environment*, 218, 245-254.

Passaro, M., S.K. Rose, O.B. Andersen, E. Boergens, F.M. Calafat, D. Dettmering, J. Benveniste, 2018b, ALES+: Adapting a homogeneous ocean retracker for satellite altimetry to sea ice leads, coastal and inland waters, *Remote Sensing of the Environment*, 211, 456-471.

Quartly, G. D.; Legeais, J.-F.; Ablain, M.; Zawadzki, L.; Fernandes, M. J.; Rudenko, S.; Carrère, L.; García, P. N.; Cipollini, P.; Andersen, O. B.; Poisson, J.-C.; Mbajon Njiche, S.; Cazenave, A.; Benveniste, J.. 2017 A new phase in the production of quality-controlled sea level data. *Earth System Science Data*, 9 (2). 557-572. <https://doi.org/10.5194/essd-9-557-2017>

Ray R.D., 2013. Precise comparisons of bottom-pressure and altimetric ocean tides, *J. Geophys. Res. Oceans*, 118, 4570-4584. <https://doi.org/10.1002/jgrc.20336>

Schaeffer, P. et al., New Mean Sea Surface CNES CLS 2015 Focusing on the use of Geodetic Missions of Cryosat-2 and Jason-1, Oral Presentation OSTST 2016



5. Annex 1: Uncertainty in Satellite estimate of Global Mean Sea Level changes, trend and acceleration - draft version

Uncertainty in Satellite estimate of Global Mean Sea Level changes, trend and acceleration

Michaël Ablain¹, Lionel Zawadzki¹, Rémi Jugier¹, Benoît Meyssignac², Aurélien Ribes³, Anny Cazenave², Nicolas Picot⁴

¹ Collecte Localisation Satellite (CLS), Ramonville Saint-Agne, 31520, France

² LEGOS, CNES, CNRS, IRD, Université Paul Sabatier, Toulouse, France

³ CNRM, Université Paul Sabatier, Météo France, CNRS, Toulouse, France

⁴ Centre National d'Etudes Spatiales (CNES), Toulouse, 31400, France

Correspondence to: Michaël Ablain (ablain.michael1@gmail.com)

Abstract. Satellite altimetry missions now provide more than 25 years of accurate, continuous and quasi-global measurements of sea level along the reference ground track of TOPEX/Poseidon. These measurements are used by different groups to build the Global Mean Sea Level (GMSL) record, an essential climate change indicator. Estimating a realistic uncertainty of the GMSL record is of crucial importance for climate studies such as estimating precisely the current rate and acceleration of sea level, analyzing the closure of the sea level budget, understanding the causes for sea level rise, detecting and attributing the response of sea level to anthropogenic activity, or estimating the Earth energy imbalance. Ablain et al., (2015) estimated the uncertainty of the GMSL trend over the period 1993-2014 by thoroughly analyzing the error budget of the satellite altimeters and showed that it amounts to ± 0.5 mm/yr (90% confidence level). In this study, we extend Ablain et al., (2015) analysis by providing a comprehensive description of the uncertainties in the satellite GMSL record. We analyse 25 years of satellite altimetry data and estimate for the first time the error variance-covariance matrix for the GMSL record with a time resolution of 10 days. Three types of errors that can affect satellite altimetry measurements are modelled (drifts, biases, noise) and combined together to derive a realistic estimate of the GMSL error variance-covariance matrix. From the error variance-covariance matrix we derive a 90% confidence envelop of the GMSL record on a 10-day basis. Then we use a least square approach and the error variance-covariance matrix to estimate the GMSL trend and acceleration uncertainties over any time periods of 5 years and longer in between October 1992 and December 2017. Over 1993-2017 we find a GMSL trend of 3.35 ± 0.4 mm/yr (90% CL) and a GMSL acceleration of 0.12 ± 0.07 mm/yr² (90% CL) in agreement (within error bars) with previous studies. The full GMSL error variance-covariance matrix is freely available online.

1 Introduction

Sea level change is a key indicator of global climate change which integrates changes in several components of the climate system in response to anthropogenic and natural forcing and also in response to internal climate variability. Since October 1992, sea level variations have been routinely measured by twelve high-precision altimeter satellites providing more than 25 years of continuous measurements. The altimeter Global Mean Sea Level (GMSL) indicator is calculated from the accurate and stable measurements of four reference altimeter missions, namely TOPEX/Poseidon (T/P), Jason-1, Jason-2 and Jason-3. All four reference missions are flying (or have flown) over the same historical ground track on a 10-day repeat cycle. They all have (or have been) precisely inter-calibrated (Zawadzki and Ablain, 2016) to ensure the long term stability of the sea level measurement. Six research groups (AVISO/CNES, SL_cci/ESA, University of Colorado, CSIRO, NASA/GSFC, NOAA) process the sea level raw data provided by satellite altimeter to estimate the GMSL time series on a 10-day basis (Figure 11). The six different estimates of the GMSL record show very small differences. The differences range between 1 and 2 mm at inter-annual time scales (1 to 5-year time scales) and between ± 0.15 mm/yr in terms of trend over the period 1993-2017. The spread across



these estimates is due to the use of different processing technique, different versions of ancillary data and different interpolation methods applied by the different groups (Henry et al., 2014; Masters et al., 2012). This spread is smaller than the real uncertainty in the sea level trend because all groups use similar methods and corrections to process the raw data and thus several sources of systematic uncertainty is not accounted for in the spread.

In a previous study (Ablain et al., 2009) proposed a realistic estimate of the uncertainty in the GMSL trend over 1993-2008 using an error budget approach. They identified the radiometer wet tropospheric correction as the main source of error. They also identified the orbit determination, the inter-calibration of altimeters and the estimate of the altimeter range, sigma-0 and significant wave height (mainly on TOPEX/Poseidon) as significant sources of error. When all terms were accounted for, they found that the uncertainty on the trend over 1993-2008 was ± 0.6 mm/yr within a 90% confidence level. This is larger than the uncertainty of ± 0.3 mm/yr over a 10-year period required by GCOS (GCOS, 2011). In the framework of the Sea Level Climate Change Initiative (SL_cci) project supported by ESA, significant improvements were made in the estimation of sea level (Ablain et al., 2015; Legeais et al., 2018; Quartly et al., 2017) to get closer to the GCOS requirements. New altimeter standards including new wet troposphere corrections, new orbit solutions, new atmospheric corrections and others were selected and applied to improve the sea level estimation. The GMSL trend uncertainties were then updated and estimated at different temporal and spatial scales (Ablain et al., 2015; Legeais et al., 2018). During the second altimetry decade, from 2002 to 2014, Ablain et al., (2015) estimated that the GMSL trend uncertainty was lower than ± 0.5 mm/yr (90% CL) for periods longer than 10 years.

In previous studies (Ablain et al., 2009; Legeais et al., 2018), the uncertainty in GMSL have been estimated for long term trends (periods of 10 years or more, that start in 1993), interannual time scales (at time scales between 1 and 5 years) and annual time scales. This estimation of the uncertainty on three different time scales is a valuable first step but it is not sufficient, as it does not fully meet the needs of the scientific community. Indeed, for many climate studies there is a need for GMSL uncertainty characterization over different time scales and over different time spans within the 25-year altimetry record. For instance, in sea level budget studies consisting in assessing the evolution of the different GMSL components, there is a need of GMSL uncertainty estimates at monthly time scales when we want to interpret GMSL monthly changes in terms of ocean mass changes (which are resolved at monthly time scales since 2002 by the gravity recovery and climate experiment –GRACE – mission). In studies that estimate the Earth energy imbalance with the sea level budget approach, this is also the case (e.g. Meyssignac et al. 2018). In detection attribution studies (e.g. Slangen et al. 2017), uncertainty in trend estimates are often needed but over different time spans than the ones addressed in Ablain et al., (2015, 2009) and in Legeais et al., (2018). Sometimes it is the uncertainty on different metrics that is needed. For example recently (Dieng et al., 2017; Nerem et al., 2018) estimated the acceleration in GMSL over 1993-2017 and found a small acceleration of ~ 0.08 mm/yr² over the 25 year-long altimetry record. There is a need for the estimation of the uncertainty in the GMSL acceleration to determine whether this acceleration is significant or not.

Note that here in this paper we address the uncertainty in the GMSL record that arises from the errors in the satellite altimetry instrument. This uncertainty can be used to quantify the measurement uncertainty on the GMSL record. This is an important piece of information for detection attribution studies that seek to estimate the GMSL rise in response to anthropogenic activity. But this is not sufficient. In detection attribution studies the response of the GMSL to anthropogenic activity need to be separated from the response of the GMSL to the natural variability of the climate system because the latter is an additional source of uncertainty. Here we not address this problem of separating the GMSL response to different sources of variability. We strictly focus on the instrument errors and the associated uncertainty.

The objective of this paper is to estimate the error variance-covariance matrix of the GMSL (on a 10-day basis) from satellite altimetry measurements. This error variance-covariance matrix provides a



comprehensive description of the uncertainties in GMSL to users. It covers all time scales that are included in the 25-year long satellite altimetry record: from 10 days (the time resolution of the GMSL time series) to multidecadal time scales. It also enables to estimate the uncertainty in any metrics derived from GMSL measurements such as trend, acceleration or other moments of higher order.

To estimate the error variance-covariance matrix, we use an error budget approach at global scale, on a 10-day basis, in which we consider all major sources of uncertainty in the altimetry measurement including the wet troposphere correction, the orbit solutions, the intercalibration of satellites and others. We also consider the temporal correlation between the different sources of uncertainty (section 2). Errors are characterized for each altimetry mission separately since different missions are affected by different sources of errors (section 2). On the basis of the error variance-covariance matrix we estimate the uncertainty in GMSL individual measurements on a 10-day basis (section 3) and the uncertainty in trend and acceleration over all periods included in the 25-year satellite altimetry record (1993-2017) (Section 4). Note that in this article all uncertainties associated to the GMSL are reported with a 90% CL unless stated otherwise. Note as well that the description of the variance-covariance matrix is given at the 1σ level.

1 GMSL data series

The six main groups that provide satellite altimetry based GMSL estimates (AVISO/CNES, SL_cci/ESA, University of Colorado, CSIRO, NASA/GSFC, NOAA) use 1-Hz altimetry measurements from T/P, Jason-1, Jason-2 and Jason-3 missions from 1993 to 2018 (1993-2015 for SL_cci/ESA). Each group process the 1-Hz data with geophysical corrections to correct the altimetry measurement for various aliasing, biases and drifts (caused for example by different atmospheric condition, different sea states, by ocean tides and others (see Ablain et al., (2009) for more details). Then they average spatially the data over each 10-day long orbital cycle to provide GMSL estimates on a 10-day basis. Differences among GMSL estimates from different groups arise from different data editing, differences in the geophysical corrections, and differences in the method used to spatially average individual measurements during orbital cycles (Henry et al., 2014; Masters et al., 2012).

Recently, comparisons of the GMSL time series derived from satellite altimetry with independent estimates based on tide gauge records (Valladeau et al., 2012; Watson et al., 2015) or on the combination of the contribution to sea level from thermal expansion, land ice melt and land water storage (Dieng et al., 2017) showed that there was a drift in the GMSL record over the period 1993-1998. This drift is caused by an erroneous onboard calibration correction on TOPEX-A (Beckley et al., 2017). The impact on the GMSL changes is -1.0 mm/yr between January 1993 and July 1995, and +3.0 mm/yr between August 1995 and February 1999, with an uncertainty of ± 1.7 mm/yr (within a 90%CL, (Ablain, 2017)).

Without taking into account the TOPEX-A drift correction, the differences between all GMSL time series are small, with maximum 1993-2017 trend differences lower than 0.15 mm/yr, representing less than 5% of the GMSL trend. The differences observed at interannual time scales are also small (<2 mm). By correcting the drift of TOPEX-A using either of the available empirical corrections (REF) the differences among solutions remain the same (the difference between empirical corrections being smaller than the difference between the raw GMSL time series). Only the GMSL trend is reduced by about 0.25 mm/yr over 1993-2017. Therefore, the choice of one or the other GMSL record is not decisive in this study, whose purpose is to characterize the uncertainties. Hereafter we use the GMSL AVISO record. The corresponding altimeter standard corrections and the GMSL processing methods are described on the AVISO website (<https://www.aviso.altimetry.fr/mssl/>).



2 Altimetry GMSL error budget

This section describes the different errors that affect the altimetry GMSL record. It builds on the GMSL error budget presented in (Ablain et al., 2009) and extends this work by taking into account new altimeter missions (Jason-2, Jason-3) and recent findings on altimetry error estimates. Three types of errors are considered: a) biases in GMSL between successive altimetry missions which are characterized by bias uncertainties ($\pm\Delta$) at a given time (t); b) drifts in GMSL characterized by a trend uncertainty ($\pm\delta$) and c) other measurement errors which exhibit time-correlation (so called residual time correlated errors here after). The residual time correlated errors are characterized by their standard deviation (σ) and correlation time scale (λ). All altimetry errors identified in this study are summarized in Table 1 and detailed hereafter. Note that all uncertainties reported in Table 1 are given at 1-sigma.

Biases can arise between the GMSL record of two successive satellite missions like between T/P and Jason-1 in May 2002, Jason-1 and Jason-2 in October 2008 and between Jason-2 and Jason-3 in October 2016. These biases are estimated during dedicated 9-month inter-calibration phases when a satellite altimeter and its successor fly over the same track, 1 minute apart. During the inter-calibration phases the bias is estimated and corrected for. Different missions show different biases but the uncertainty in the bias correction is the same for all inter-calibration phases and amounts: ± 0.5 mm (Zawadzki and Ablain, 2016). The situation is different for the switch from TOPEX altimeter side-A to side-B in February 1999 because it was impossible to do any inter-calibration phase between the two sides of TOPEX (as both instruments were flying on the same spacecraft). For the switch from TOPEX side-A to side-B we assume that the uncertainty in GMSL is greater and is about 2 mm (Zawadzki and Ablain, 2016).

Drifts may occur in the GMSL record because of drifts in the TOPEX side-A and side-B radar instruments, because of drifts in the International Terrestrial Reference Frame (ITRF) realization in which altimeter orbits are determined or because of drifts in the Glacial Isostatic Adjustment (GIA) correction applied to the GMSL record. As explained before the TOPEX side-A record shows a spurious drift due to an erroneous onboard calibration correction of TOPEX side-A (Beckley et al., 2017). This drift is corrected by different empirical approaches (Ablain, 2017; Beckley et al., 2017; Dieng et al., 2017) that are all affected by a significant uncertainty. With a comparison against an independent GMSL estimate based on tide gauge records (Ablain, 2017), we estimate this uncertainty to be ± 0.7 mm/yr (1 σ level) over the TOPEX-A period (1993-1998). For the TOPEX-B record, no GMSL drift has been reported, but (Ablain et al., 2012) showed significant Sigma-0 instabilities of the order of 0.1 dB, which generates through the sea-state bias correction an uncertainty of ± 0.1 mm/yr (1 σ level) in the GMSL record over the TOPEX-B period (February 1999-April 2002). Concerning the ITRF realization, (Couhert et al., 2015) showed that the uncertainty on the ITRF realization drift generates an uncertainty of ± 0.1 mm/yr (1 σ level) on the GMSL trend over 1993-2015. We adopt this value here for the whole period 1993-2017. For the uncertainty on the GIA correction applied to the GMSL, we use the value of 0.05 mm/yr (1 σ level) over the altimetry period from Spada (2017). Combining the uncertainty on the GMSL trend over 1993-2017 from GIA and ITRF and assuming that they are not correlated yield an uncertainty on the GMSL trend of 0.12 mm/yr over 1993-2017 (1 σ level).

Residual residual time correlated errors are separated into two different groups depending on their correlation time scales. The first group gathers the residual time correlated errors with short correlation time scales i.e. lower than 2 months and between 2 months and 1 year. The second group gathers the residual time correlated errors with long correlation time scales between 5 and 10 years. In the first group errors are mainly due to the geophysical corrections (e.g. ocean tides, atmospheric corrections, ...), the altimeter corrections (e.g. sea-state bias correction, altimeter ionospheric corrections), the orbit calculation, and potential altimeter instabilities (e.g. altimeter range and sigma-0 instabilities). At time scales below 1 year, the variability of the corrections' time series is dominated by errors such that the variance of the error in each correction is estimated by the variance of the correction's time series.. For errors with correlation time scales lower than 2 months, we estimate the



standard deviation (σ) of the error from the correction's time series filtered with a 2-month high-pass filter. As the standard deviation of the errors depends on the different altimeter missions, the standard deviation has been estimated separately for each altimeter mission. We find $\sigma = 1.7$ mm over the T/P period, $\sigma = 1.5$ mm over the Jason-1 period, and $\sigma = 1.2$ mm for Jason-2/3 period. For errors with correlation time scale between 2 months and 1 year, we used the same approach and filtered the correction time series with a pass-band filter. In this case we find $\sigma = 1.3$ mm over the T/P period, $\sigma = 1.2$ mm over the Jason-1 period, and $\sigma = 1.0$ mm for Jason-2/3 period. Not surprisingly, the highest standard deviations are obtained for T/P, and the lowest ones for Jason-2/3. This is because of larger altimeter range instabilities in T/P (Ablain et al., 2012; Beckley et al., 2017), because of the presence of a 59-day signal error on the altimeter range of T/P (Zawadzki et al., 2018), and because of the deterioration in the performance of atmospheric corrections in the early years of the altimetry era (Legeais et al., 2014). Note that Jason-1 shows also higher errors than Jason-2 and Jason-3 at time scales below 1 year (Couhert et al., 2015).

In the second group of residual time correlated errors, errors are due to errors in the on-board microwave radiometer calibration that yield instabilities in the wet troposphere correction, and also to long-term errors in the orbit calculation (Couhert et al., 2015). Because these errors are correlated at time scale longer than 5 years they can not be estimated with the standard deviation of the correction time series, the correction time series being too short (25-year long) to sample the time correlation. For this group of residual time correlated errors we use simple models to represent the time correlation of the errors with time. For the wet troposphere correction, several studies (Fernandes et al., 2015; Legeais et al., 2014; Thao et al., 2014) have identified long-term differences among the corrections computed from the different microwave radiometers and from different atmospheric reanalyses (e.g. ERA-interim reanalyzes (Dee et al., 2011)). These studies report a difference in the wet tropospheric correction for GMSL in the range of 0.2-0.3 mm/yr for period of 5 to 10 years. In this error budget approach, we adopt a conservative approach and we model the error in wet tropospheric correction with a correlated error at 5 years with a standard deviation of 1.2 mm (1 σ level). The correlation is modeled with a gaussian attenuation based on the wavelength of the errors: $e^{-\frac{1}{2}(\frac{t}{\lambda})^2}$ with $\lambda = 5$ years. In terms of trends, this residual time correlated error generates an uncertainty of ± 0.2 mm/yr over 5-year periods. For the error in the orbit calculation, comparisons of different orbit solutions showed differences of 0.05 mm/yr on 10 year time scales due to errors in the modelling of the Earth time varying gravity field (Couhert et al., 2015). We model this error with a correlated error at 10-year time scale with a standard deviation of 0.5 mm (1 σ level). The correlation is modeled by the same gaussian attenuation with $\lambda = 10$ years. In terms of trends, it corresponds to an uncertainty of ± 0.05 mm/yr over 10-year periods.

In the next section these different terms of the GMSL error budget are combined together to build the error variance-covariance matrix. Note that the different terms of the altimeter GMSL error budget described here are based on the current knowledge of altimetry measurement errors. As the altimetry record increases in length with new altimeter missions, the knowledge of the altimetry measurement also increases, and the description of the errors improves. This implies that the error variance-covariance matrix is expected to improve and change in the future.

3 The GMSL error variance-covariance matrix

In this section we derive the error variance-covariance matrix (Σ) of the GMSL from the error budget described in section 2. Then we derive from Σ the uncertainty of each single GMSL measurement (made every 10 days) and plot the associated GMSL uncertainty envelope.

We assume that all error sources presented in Table 1 are independent from each other. Thus the Σ matrix is the sum of the individual variance-covariance matrix of each error source Σ_i in the error budget (see Figure 12). Each Σ_i matrix is calculated from a large number of random draws (> 1000) of simulated error signal using the model described in section 2 (either a bias, drift or time correlated signal) fed with a standard normal distribution.

The resulting shape of each individual Σ_i matrix depends on the type of error (bias, drift or time correlated signal, see Figure 12). For biases, the Σ_i matrix takes the shape of constant square blocks each side of the time occurrence of the bias correction (see for example the square matrix for TOPEX-A and TOPEX-B on the low left corner of Figure 12 along the diagonal). This shape in square blocks



means that the error in the bias correction generates an error on the GMSL which is fully correlated along time before and after the bias correction time, but which is not correlated along time for dates that are apart of the bias correction time. This is consistent with what we expect from a bias correction error. Note that in this article (and in climate change studies in general) we are interested only in GMSL changes, trends or acceleration but not on the time mean GMSL (which is the absolute reference of GMSL). Thus, we have removed from the GMSL time series the temporal mean over 1993-2017. The reference of the GMSL is thus arbitrary and assumed to be perfectly known. This is the reason why the reference of the GMSL is not affected by the biases correction error here.

For drifts, the Σ_i matrix take the shape of a horse saddle. This is because an error on the GMSL drift over a given period generates errors on the GMSL time series which are correlated when they are close in time and anti-correlated when they are on opposite side of the drift period.

For residual time correlated errors, the Σ_i matrix take the shape of a diagonal matrix with off diagonal terms of smaller amplitude. The more the off-diagonal terms are far from the diagonal the more they are attenuated. The attenuation rate is a Gaussian attenuation based on the wavelength of the time correlated errors ($e^{-\frac{1}{2}(\frac{t}{\lambda})^2}$), with various time-scales λ .

All individual Σ_i matrix are summed up together to build the total error variance-covariance matrix Σ of the altimetry-derived continuous GMSL record (corrected for TOPEX-A drift) over 1993-2018 (see Figure 12). As expected, the dominant terms of the matrix are on the diagonal. They are largely due to the different sources of errors with correlation time scales below 1 year (first group of errors in section 2). The diagonal terms are the highest at the beginning of the altimetry period when T/P was at work. This is because of larger altimeter range instabilities in T/P, the presence of a 59-day signal error on the altimeter range of T/P and poorer performance of atmospheric corrections in the early years of the altimetry era (Legeais et al., 2014). The dominant off-diagonal terms are also found during the T/P period (in the lower left corner of the matrix, see Figure 12). The terms are induced by the TOPEX-A trend error and the large bias correction uncertainty between TOPEX-A and TOPEX-B (because of the absence of inter-calibration phase between T/P side-A and T/P side-B).

4 GMSL uncertainty envelope

We estimate the GMSL uncertainty envelope from the square root of the diagonal terms of Σ (see Figure 13). As expected, the GMSL time series shows a larger uncertainty during the T/P period (5 mm to 8 mm) than during the Jason period (close to 4 mm). The bias correction uncertainty between TOPEX side-A and TOPEX side-B in February 1999 is also clearly visible with a 1-mm drop in the uncertainty after the switch to TOPEX side-B. Note that the uncertainty envelope has a parabolic shape and shows smaller uncertainties during the beginning of the Jason-2 period (3.5 mm around 2008) than over the Jason-3 period (4.5 mm). This is not because Jason-1 and Jason-2 errors are smaller than Jason-3's errors. Actually Jason 2 and Jason-3 errors are slightly smaller than Jason-1 errors thanks to better orbit determination. The uncertainties are smaller during the Jason-1 and Jason-2 period because this period is in the center of the record. It benefits from prior and posterior data that covariate and help in reducing the uncertainty when they are combined together. In contrast the Jason-3 period is located at the end of the record and does not benefits from posterior data to help reduce the uncertainty.

On Figure 14 we superimpose the GMSL time series (average of the GMSL time series in Figure 11) and the associated uncertainty envelop. For the TOPEX-A period we test 3 different curve with three different corrections based on the removal of the Cal-1 mode (Beckley et al., 2017), the comparison with tide gauges (Ablain, 2017; Watson et al., 2015), or based on a sea level closure budget approach (Dieng et al., 2017). Figure 14The uncertainty envelop is centered on the record corrected for T/P side-A drift with the correction based on (Ablain et al., 2017). As expected, all empirically corrected GMSL records are within the uncertainty envelop.



5 Uncertainty in GMSL trend and acceleration

The variance-covariance matrix can be used to derive the uncertainty on any metric based on the GMSL time series. In this section we use the error variance-covariance matrix to estimate the uncertainty on the GMSL trend and the GMSL acceleration over any period of 5 years and more within 1993-2017.

Recently, several studies (Dieng et al., 2017; Nerem et al., 2018; Watson et al., 2015; WCRP Global Sea Level Budget Group, 2018) found a significant acceleration in the GMSL record from satellite altimetry (after correction of the TOPEX side-A drift) of 0.08-0.12 mm/yr². The presence of an acceleration in the record should not change the estimation of the trend when estimated with a least square approach. However it can affect the estimation of the uncertainty on the trend. To cope with this issue we address here at the same time the estimation of the trend and the estimation of the acceleration in the GMSL record. To this objective we use a second order polynomial as predictor. Considering the GMSL record has n observations, let X be an $n \times 3$ predictor where the first column contains only ones (representing the constant term), the second column contains the time vector (representing the linear term) and the third column contains the square of the time vector (representing the squared term). Let y be an $n \times 1$ vector of independent observations of the GMSL. Let ϵ be an $n \times 1$ vector of disturbances (GMSL non-linear and non-quadratic signals) and errors. Let β be the 3×1 vector of unknown parameters that we want to estimate, namely the GMSL y-intercept, the GMSL trend and the GMSL acceleration. Our linear regression model for the estimation of the GMSL trend and acceleration will thus be

$$y = X\beta + \epsilon.$$

with

$$\epsilon \sim N(0, \Sigma)$$

where Σ is the variance-covariance matrix of the observation errors (estimated in the previous section) which is different from the identity because of the correlated noise (see section 2).

The most commonly used method to estimate the GMSL trend and acceleration is the Ordinary Least Squares (OLS) estimator in its classical form (Cazenave and Llovel, 2010; Dieng et al., 2015; Masters et al., 2012; Nerem et al., 2018). This is also the most common method to estimate trends and accelerations in other climate essential variable (Hartmann et al., 2013, and references therein). For this reason we turn here to the OLS to fit the linear regression model. The estimator of β with the OLS approach, noted $\hat{\beta}$ is

$$\hat{\beta} = (X^t X)^{-1} X^t y.$$

In most cases, ϵ follows a $N(0, \sigma^2 I)$ distribution, which implies that $\hat{\beta}$ follows a Normal Law

$$\hat{\beta} = N(\beta, \sigma^2 (X^t X)^{-1})$$

The issue with this common framework is that the uncertainty of the trend and acceleration estimates does not take into account the correlated errors of the GMSL observations.

To **address this issue**, we use a more general formalism to integrate the GMSL error in the trend uncertainty estimation, following (Ablain et al., 2009; Ribes et al., 2016), and IPCC AR5 (Hartmann et al., 2013, see in particular Box 2.2 and Supplementary Material). The OLS estimator is left unchanged (and is still unbiased), but its distribution is revised to account for Σ , leading to:

$$\hat{\beta} = N(\beta, (X^t X)^{-1} (X^t \Sigma X) (X^t X)^{-1})$$

Note that this estimate is known to be less accurate than the General Least Square estimate (GLS, which is the optimal estimator in the case where $\Sigma \neq I$) in terms of the mean square error, because its variance is larger. A generalized least square estimate would probably help in narrowing slightly the trend uncertainty but the difference would likely be small as the GMSL time series is almost linear in time. Important advantages of using OLS here are (i) OLS is consistent with previous estimators of



GMSL trends as well as estimators of trends in other essential climate variable than GMSL (e.g. Hartmann et al., 2013), and (ii) the OLS best-estimate does not depend on the estimated variance-covariance matrix Σ .

Based on the matrix Σ defined in the previous section, and the OLS solution proposed before, we now estimate the GMSL trend (mm/yr) and acceleration (mm/yr²) uncertainties for any time span included in the period 1993-2017. Results are synthetically displayed in

Figure 15 for trends and in Figure 16 for accelerations. On Figure 5, The top of the triangle indicates that the GMSL trend uncertainty over 1993-2017 is ± 0.4 mm/yr (CL 90%, Figure 5

Figure 15) and that the GMSL acceleration uncertainty over the same period is ± 0.07 mm/yr² (CL 90%, Figure 16). The GMSL acceleration uncertainty estimate is consistent with results of Watson et al. (2015), on the January 1993 to June 2014 time period where they find an uncertainty of $\pm 0.058 \text{ mm.yr}^{-2}$ at 1σ which corresponds to ± 0.096 mm/yr² at the 90% confidence level. This is slightly larger than Nerem et al. (2018) estimate which is ± 0.025 mm/yr² at 1σ on the full 25-year altimetry era which corresponds to 0.041 mm/yr² at 90% confidence level. But Nerem et al. (2018) estimate is likely underestimated as they only consider omission errors. The GMSL acceleration uncertainties have been calculated for all periods of 10 years and more within 1993-2017 (Figure 16). As expected, uncertainties tend to increase when the period length decreases. At 10 years, the GMSL acceleration uncertainties are ranging from ± 0.3 mm/yr² over the T/P period to ± 0.25 mm/yr² over the Jason era. At 20 years they range between ± 0.12 and ± 0.08 mm/yr².

A cross-sectional analysis of the 10-year horizontal line on Figure 5 shows that the GMSL trend uncertainties over 10 years periods decreased from 1.0 mm/yr over the first decade to 0.5 mm/yr over the last one. The larger uncertainty over the first decade is mainly due to the TOPEX-A drift error but also to the large intermission bias uncertainty between TOPEX-A and TOPEX-B and to a lesser extent to the improvement of GMSL accuracy with Jason-2 and Jason-3. Note that the current GCOS requirement of 0.3 mm/yr uncertainty over 10 years (GCOS, 2011) is not met at the 90% confidence level. But the recent record over the last decade based on the Jason series is close to meet the GCOS requirement. Figure 5 can also be analysed by following the sides of the triangle. The results of this analysis are plotted on Figure 17 **Erreur ! Source du renvoi introuvable.** The plain line corresponds to the left side, read from bottom left to the top of the triangle. The dashed line corresponds to the right side, read from bottom right to the top. As expected, both curves show a reduction of the trend uncertainty as the period over which trends are computed increases from 2 to 25 years. The difference between the two lines shows the reduction of GMSL errors thanks to the improvement of the measurement in latest altimetry missions. The lowest trend uncertainty is obtained with the last 20 years of the GMSL record: 0.35 mm/yr.

Figure 8 indicates the periods for which the acceleration in sea level is significant at the 90% confidence level. The acceleration is visible at the end of the record for periods of 10 years and longer. The GMSL acceleration is 0.12 mm/yr² with an uncertainty of 0.07 mm/yr² at 90% confidence level over the 25-year altimetry era. This proves that the acceleration observed in the GMSL evolution is statistically significant. It is worth noting that the different empirical TOPEX-A corrections yield very similar results (0.126 mm/yr² (Ablain, 2017) ; 0.120 mm/yr² (Dieng et al., 2017; Watson et al., 2015), 0.114 mm/yr² (Beckley et al., 2017). This acceleration at the end of the record is due to an acceleration in the contribution to sea level from Greenland and from other contributions but to a lesser extent (Dieng et al. 2017, Chen et al. 2017, Nerem et al. 2018). A small acceleration is also visible during the period 1993-2005 at the beginning of the record. This acceleration is likely due to the recovery from the Mount Pinatubo eruption in 2011 (Fasullo et al. 2016).

Figure 9 indicates the period for which the trend in sea level is significant at the 90% confidence level. In periods where the acceleration is not significant the second order polynomial that we used as predictor to estimate the trend and the acceleration does not hold anymore in principle. For these



periods we should turn to a first order polynomial. The use of a first order polynomial does not affect the trend estimates. It only affects the trend uncertainty estimates. We checked for differences in trend uncertainty when using either second order or first order polynomial predictors. We found that the differences are negligible (not shown).. Figure 9 indicates that for periods of 5 years and longer the trend in GMSL is always significant at 90% CL over the whole record. At the end of the record the trend tend to increase which is consistent with the acceleration plot on Figure 6. Over the 25 years of satellite altimetry we find a sea level rise of 3.35 ± 0.4 mm/yr (90% CL), after correcting for the TOPEX-A GMSL drift. The differences due to the different TOPEX A corrections is negligible (<0.05 mm.yr⁻¹)

6 Conclusions

In this study we have estimated the full GMSL error variance-covariance matrix over the satellite altimetry period. The matrix is available online (see section data). It provides to users a comprehensive description of the GMSL errors over the altimetry period. This matrix is based on the current knowledge of altimetry measurement errors. As the altimetry record increases in length with new altimeter missions, the knowledge of the altimetry measurement also increases, and the description of the errors improves. Consequently the error variance-covariance matrix is expected to change and improve in the future – hopefully with a reduction of measurement uncertainty in new products.

The uncertainty of the GMSL computed here shows the reliability of altimetry measurements to accurately describe the evolution of the GMSL on all time scales from 10 days to 25 years.. It also shows the reliability of altimetry measurements to estimate sea level trends and now accelerations. Along the altimetry record, we find that the uncertainty in each individual GMSL measurement decreases with time. It is smaller during the Jason era (2002-2018) than during the T/P period (1993-2002). Over the entire altimetry record, 1993-2017, we estimate the GMSL trend to 3.35 ± 0.4 mm/yr (90% CL, after correcting the TOPEX-A GMSL drift). We detect also a significant GMSL acceleration over the 25-year period at 0.12 ± 0.07 mm/yr² (90% CL).

Several assumptions have been made in this study that could be improved in the futur. First, the modelling of altimeter errors should be regularly revisited and improved to take into account a better knowledge of errors (e.g stability of wet troposphere corrections) and to consider future altimeter missions (e.g. Sentinel-3 and Sentinel-6 missions). With regards to the mathematical formalism, OLS method has been applied because it is the most common approach used in the climate community to calculate trends in any climate data records. However this is not the optimal linear estimator. The use of a Generalized Least Square approach should involve some narrowing of trend or acceleration uncertainty. Another topic of concerns is the consideration of the internal and forced variability of the GMSL. Here we only considered the uncertainty in the GMSL due to the satellite altimeter instrument. In a future study it would be interesting to consider the partition of the GMSL into the forced response to anthropogenic forcing and the natural response to natural forcing and to the internal variability. Estimating the natural GMSL variability (e.g. using models) and considering it as an additional residual time correlated error, would allow to calculate the GMSL trend and acceleration representing the long-term evolution of GMSL in relationship with climate change.

Data

The global mean sea level error variance-covariance matrix is available online at <https://doi.org/10.17882/58344>



Acknowledgment

This work was carried out as part of the Sea level CCI (SL_cci) project (Climate Change Initiative program) supported by ESA and the SALP (Service d'Altimétrie et de Localisation Précise) project supported by CNES for several years. We would also like to thank all contributors to these two projects, with special recognition to Jérôme Benveniste, technical officer of the SL_cci project at ESA, and Thierry Guinle, SALP project manager at CNES.

References

- Ablain, M., 2017. The TOPEX-A Drift and Impacts on GMSL Time Series. Presented at the OSTST, https://meetings.aviso.altimetry.fr/fileadmin/user_upload/tx_ausyclsseminar/files/Poster_OSTST17_GMSL_Drift_TOPEX-A.pdf, Miami, US (October, 2017).
- Ablain, M., Cazenave, A., Larnicol, G., Balmaseda, M., Cipollini, P., Faugère, Y., Fernandes, M.J., Henry, O., Johannessen, J.A., Knudsen, P., Andersen, O., Legeais, J., Meyssignac, B., Picot, N., Roca, M., Rudenko, S., Scharffenberg, M.G., Stammer, D., Timms, G., Benveniste, J., 2015. Improved sea level record over the satellite altimetry era (1993–2010) from the Climate Change Initiative project. *Ocean Science* 11, 67–82. <https://doi.org/10.5194/os-11-67-2015>
- Ablain, M., Cazenave, A., Valladeau, G., Guinehut, S., 2009. A new assessment of the error budget of global mean sea level rate estimated by satellite altimetry over 1993–2008. *Ocean Science* 5, 193–201. <https://doi.org/10.5194/os-5-193-2009>
- Ablain, M., Legeais, J.F., Prandi, P., Marcos, M., Fenoglio-Marc, L., Dieng, H.B., Benveniste, J., Cazenave, A., 2017. Satellite Altimetry-Based Sea Level at Global and Regional Scales. *Surveys in Geophysics* 38, 7–31. <https://doi.org/10.1007/s10712-016-9389-8>
- Ablain, M., Philipps, S., Urvoy, M., Tran, N., Picot, N., 2012. Detection of Long-Term Instabilities on Altimeter Backscatter Coefficient Thanks to Wind Speed Data Comparisons from Altimeters and Models. *Marine Geodesy* 35, 258–275. <https://doi.org/10.1080/01490419.2012.718675>
- Beckley, B.D., Callahan, P.S., Hancock, D.W., Mitchum, G.T., Ray, R.D., 2017. On the “Cal-Mode” Correction to TOPEX Satellite Altimetry and Its Effect on the Global Mean Sea Level Time Series: TOPEX CAL-MODE CORRECTION AND SEA LEVEL. *Journal of Geophysical Research: Oceans* 122, 8371–8384. <https://doi.org/10.1002/2017JC013090>
- Cazenave, A., Llovel, W., 2010. Contemporary Sea Level Rise. *Annual Review of Marine Science* 2, 145–173. <https://doi.org/10.1146/annurev-marine-120308-081105>
- Couhert, A., Cerri, L., Legeais, J.-F., Ablain, M., Zelensky, N.P., Haines, B.J., Lemoine, F.G., Bertiger, W.I., Desai, S.D., Otten, M., 2015. Towards the 1mm/y stability of the radial orbit error at regional scales. *Advances in Space Research* 55, 2–23. <https://doi.org/10.1016/j.asr.2014.06.041>
- Dee, D.P., Uppala, S.M., Simmons, A.J., Berrisford, P., Poli, P., Kobayashi, S., Andrae, U., Balmaseda, M.A., Balsamo, G., Bauer, P., Bechtold, P., Beljaars, A.C.M., van de Berg, L., Bidlot, J., Bormann, N., Delsol, C., Dragani, R., Fuentes, M., Geer, A.J., Haimberger, L., Healy, S.B., Hersbach, H., Hólm, E.V., Isaksen, I., Kållberg, P., Köhler, M., Matricardi, M., McNally, A.P., Monge-Sanz, B.M., Morcrette, J.-J., Park, B.-K., Peubey, C., de Rosnay, P., Tavolato, C., Thépaut, J.-N., Vitart, F., 2011. The ERA-Interim reanalysis: configuration and performance of the data assimilation system. *Quarterly Journal of the Royal Meteorological Society* 137, 553–597. <https://doi.org/10.1002/qj.828>
- Dieng, H.B., Cazenave, A., Meyssignac, B., Ablain, M., 2017. New estimate of the current rate of sea level rise from a sea level budget approach: SEA LEVEL BUDGET. *Geophysical Research Letters* 44, 3744–3751. <https://doi.org/10.1002/2017GL073308>
- Dieng, H.B., Cazenave, A., von Schuckmann, K., Ablain, M., Meyssignac, B., 2015. Sea level budget over 2005–2013: missing contributions and data errors. *Ocean Sci.* 11, 789–802. <https://doi.org/10.5194/os-11-789-2015>



Fernandes, M.J., Lázaro, C., Ablain, M., Pires, N., 2015. Improved wet path delays for all ESA and reference altimetric missions. *Remote Sensing of Environment* 169, 50–74. <https://doi.org/10.1016/j.rse.2015.07.023>

GCOS, 2011. Systematic Observation Requirements for Satellite-Based Data Products for Climate (2011 Update) – Supplemental details to the satellite-based component of the “Implementation Plan for the Global Observing System for Climate in Support of the UNFCCC (2010 Update) (No. GCOS-154), GCOS- No. 154. WMO.

Hartmann, D.L., A.M.G. Klein Tank, M. Rusticucci, L.V. Alexander, S. Brönnimann, Y. Charabi, F.J. Dentener, E.J. Dlugokencky, D.R. Easterling, A. Kaplan, B.J. Soden, P.W. Thorne, M. Wild and P.M. Zhai, 2013: Observations: Atmosphere and Surface. In: *Climate Change 2013: The Physical Science Basis. Contribution of Working Group I to the Fifth Assessment Report of the Intergovernmental Panel on Climate Change* [Stocker, T.F., D. Qin, G.-K. Plattner, M. Tignor, S.K. Allen, J. Boschung, A. Nauels, Y. Xia, V. Bex and P.M. Midgley (eds.)]. Cambridge University Press, Cambridge, United Kingdom and New York, NY, USA.

Henry, O., Ablain, M., Meyssignac, B., Cazenave, A., Masters, D., Nerem, S., Garric, G., 2014. Effect of the processing methodology on satellite altimetry-based global mean sea level rise over the Jason-1 operating period. *Journal of Geodesy* 88, 351–361. <https://doi.org/10.1007/s00190-013-0687-3>

Legeais, J.-F., Ablain, M., Thao, S., 2014. Evaluation of wet troposphere path delays from atmospheric reanalyses and radiometers and their impact on the altimeter sea level. *Ocean Science* 10, 893–905. <https://doi.org/10.5194/os-10-893-2014>

Legeais, J.-F., Ablain, M., Zawadzki, L., Zuo, H., Johannessen, J.A., Scharffenberg, M.G., Fenoglio-Marc, L., Fernandes, M.J., Andersen, O.B., Rudenko, S., Cipollini, P., Quartly, G.D., Passaro, M., Cazenave, A., Benveniste, J., 2018. An improved and homogeneous altimeter sea level record from the ESA Climate Change Initiative. *Earth System Science Data* 10, 281–301. <https://doi.org/10.5194/essd-10-281-2018>

Llovel, W., Willis, J.K., Landerer, F.W., Fukumori, I., 2014. Deep-ocean contribution to sea level and energy budget not detectable over the past decade. *Nature Climate Change* 4, 1031.

Masters, D., Nerem, R.S., Choe, C., Leuliette, E., Beckley, B., White, N., Ablain, M., 2012. Comparison of Global Mean Sea Level Time Series from TOPEX/Poseidon, Jason-1, and Jason-2. *Marine Geodesy* 35, 20–41. <https://doi.org/10.1080/01490419.2012.717862>

Nerem, R.S., Beckley, B.D., Fasullo, J.T., Hamlington, B.D., Masters, D., Mitchum, G.T., 2018. Climate-change-driven accelerated sea-level rise detected in the altimeter era. *PNAS* 201717312. <https://doi.org/10.1073/pnas.1717312115>

Quartly, G.D., Legeais, J.-F., Ablain, M., Zawadzki, L., Fernandes, M.J., Rudenko, S., Carrère, L., Garcia, P.N., Cipollini, P., Andersen, O.B., Poisson, J.-C., Mbajon Njiche, S., Cazenave, A., Benveniste, J., 2017. A new phase in the production of quality-controlled sea level data. *Earth System Science Data* 9, 557–572. <https://doi.org/10.5194/essd-9-557-2017>

Ribes, A., Corre, L., Gibelin, A.-L., Dubuisson, B., 2016. Issues in estimating observed change at the local scale - a case study: the recent warming over France: ESTIMATING OBSERVED WARMING AT THE LOCAL SCALE. *International Journal of Climatology* 36, 3794–3806. <https://doi.org/10.1002/joc.4593>

Rudenko, S., Neumayer, K.-H., Dettmering, D., Esselborn, S., Schone, T., Raimondo, J.-C., 2017. Improvements in Precise Orbits of Altimetry Satellites and Their Impact on Mean Sea Level Monitoring. *IEEE Transactions on Geoscience and Remote Sensing* 55, 3382–3395. <https://doi.org/10.1109/TGRS.2017.2670061>

Slangen, A.B.A., Adloff, F., Jevrejeva, S., Leclercq, P.W., Marzeion, B., Wada, Y., Winkelmann, R., 2017. A Review of Recent Updates of Sea-Level Projections at Global and Regional Scales. *Surveys in Geophysics* 38, 385–406. <https://doi.org/10.1007/s10712-016-9374-2>

Spada, G., 2017. Glacial Isostatic Adjustment and Contemporary Sea Level Rise: An Overview. *Surveys in Geophysics* 38, 153–185. <https://doi.org/10.1007/s10712-016-9379-x>



- Thao, S., Eymard, L., Obligis, E., Picard, B., 2014. Trend and Variability of the Atmospheric Water Vapor: A Mean Sea Level Issue. *Journal of Atmospheric and Oceanic Technology* 31, 1881–1901. <https://doi.org/10.1175/JTECH-D-13-00157.1>
- Valladeau, G., Legeais, J.F., Ablain, M., Guinehut, S., Picot, N., 2012. Comparing Altimetry with Tide Gauges and Argo Profiling Floats for Data Quality Assessment and Mean Sea Level Studies. *Marine Geodesy* 35, 42–60. <https://doi.org/10.1080/01490419.2012.718226>
- von Schuckmann, K., Palmer, M.D., Trenberth, K.E., Cazenave, A., Chambers, D., Champollion, N., Hansen, J., Josey, S.A., Loeb, N., Mathieu, P.-P., Meyssignac, B., Wild, M., 2016. An imperative to monitor Earth's energy imbalance. *Nature Climate Change* 6, 138.
- Watson, C.S., White, N.J., Church, J.A., King, M.A., Burgette, R.J., Legresy, B., 2015. Unabated global mean sea-level rise over the satellite altimeter era. *Nature Climate Change* 5, 565–568. <https://doi.org/10.1038/nclimate2635>
- WCRP Global Sea Level Budget Group, 2018. Global sea-level budget 1993–present. *Earth System Science Data* 10, 1551–1590. <https://doi.org/10.5194/essd-10-1551-2018>
- Zawadzki, L., Ablain, M., 2016. Accuracy of the mean sea level continuous record with future altimetric missions: Jason-3 vs. Sentinel-3a. *Ocean Sci.* 12, 9–18. <https://doi.org/10.5194/os-12-9-2016>
- Zawadzki, L., Ablain, M., Carrere, L., Ray, R.D., Zelensky, N.P., Lyard, F., Guillot, A., Picot, N., 2018. Investigating the 59-Day Error Signal in the Mean Sea Level Derived From TOPEX/Poseidon, Jason-1, and Jason-2 Data With FES and GOT Ocean Tide Models. *IEEE Transactions on Geoscience and Remote Sensing* 56, 3244–3255. <https://doi.org/10.1109/TGRS.2018.2796630>

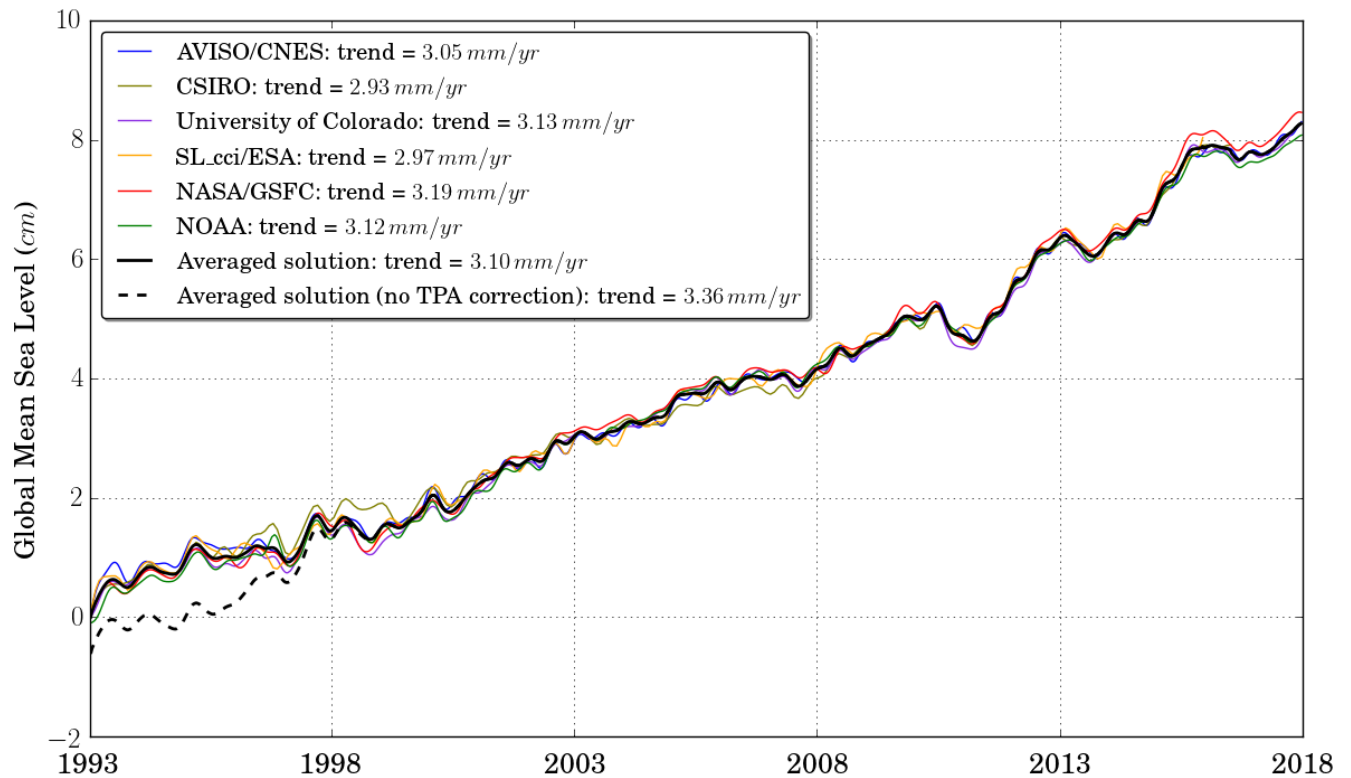


Figure 11: Evolution of GMSL time series (corrected for TOPEX-A drift using (Ablain, 2017) TOPEX-A correction) from 6 different groups (AVISO/CNES, CSIRO, University of Colorado, SL_cci/ESA, NASA/GSFC, NOAA) products. The SL_cci/ESA covers period January 1993 to December 2016 while all other products cover the full 25-year period (January 1993 to December 2018). Seasonal (annual and semi-annual) signals have been removed and a 6-month smoothing is applied. An averaged solution is computed from the 6 groups. GMSL time series have the same average on the 1993-2015 period (common period) and the averaged solution starts at 0 in 1993. The average solution without TOPEX-A correction is also represented. A GIA correction of -0.3 mm/yr has been subtracted to each data set.

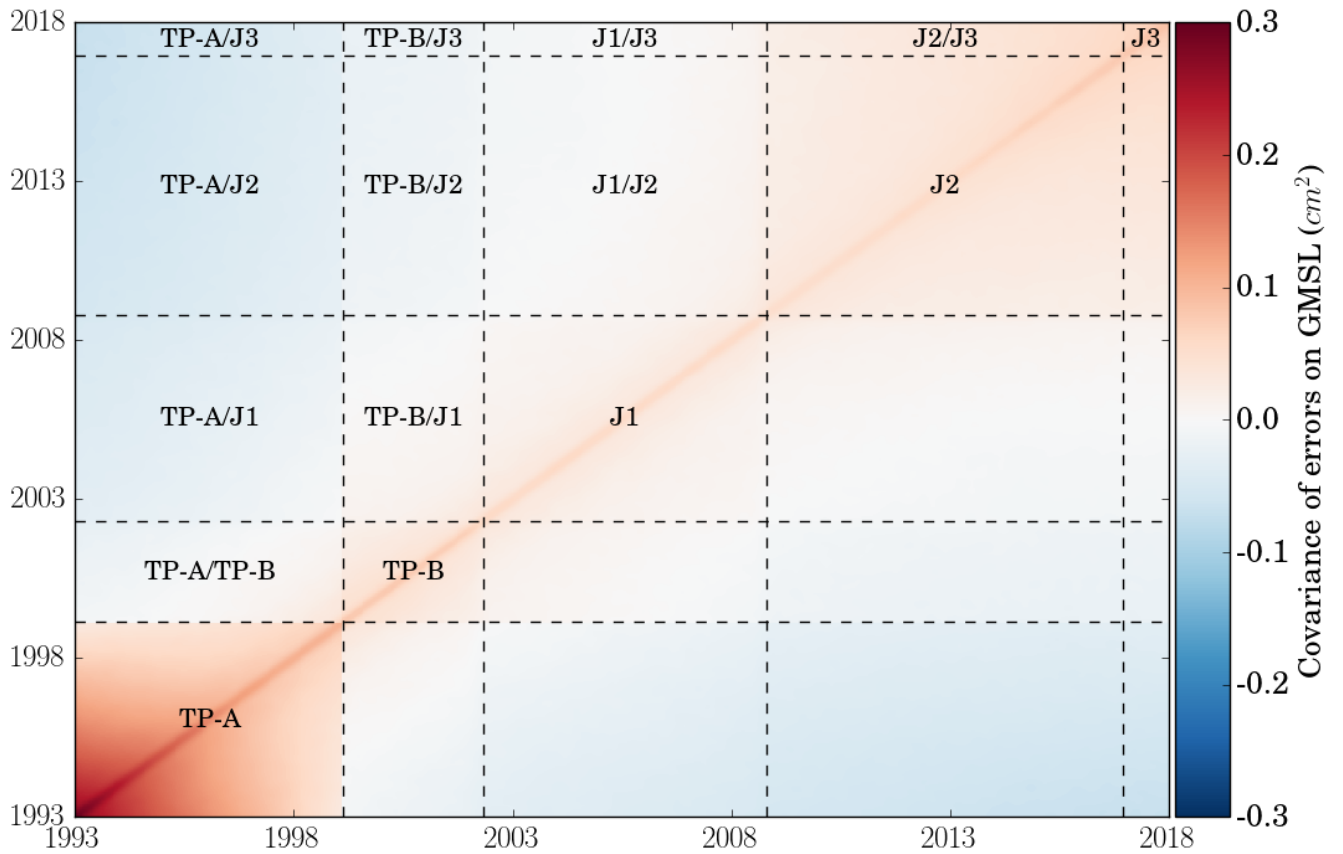


Figure 12: Error variance-covariance matrix of altimeter GMSL on the 25-years period (January 1993 to December 2017).

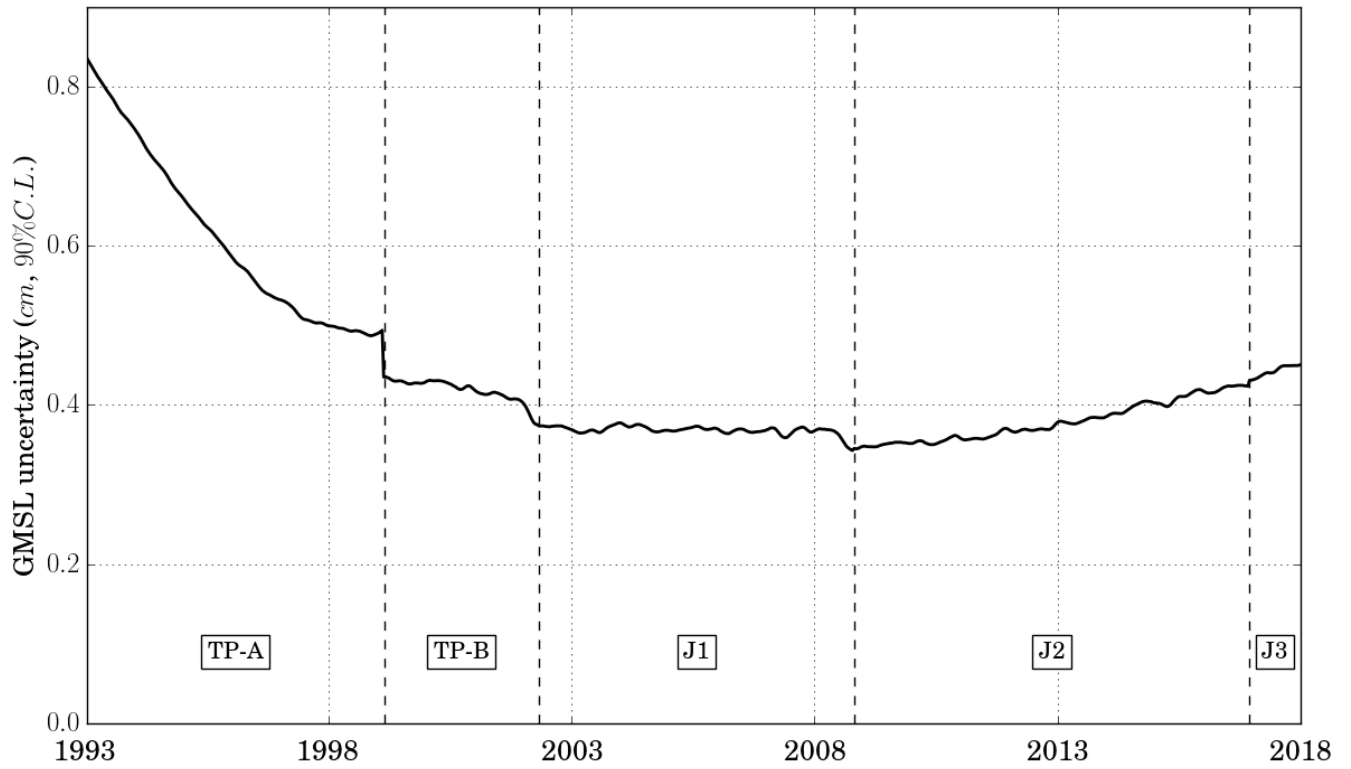


Figure 13: Evolution on time of GMSL measurement uncertainty within a 90 % confidence level (i.e. 1.65σ) on the 25-years period (January 1993 to December 2017).

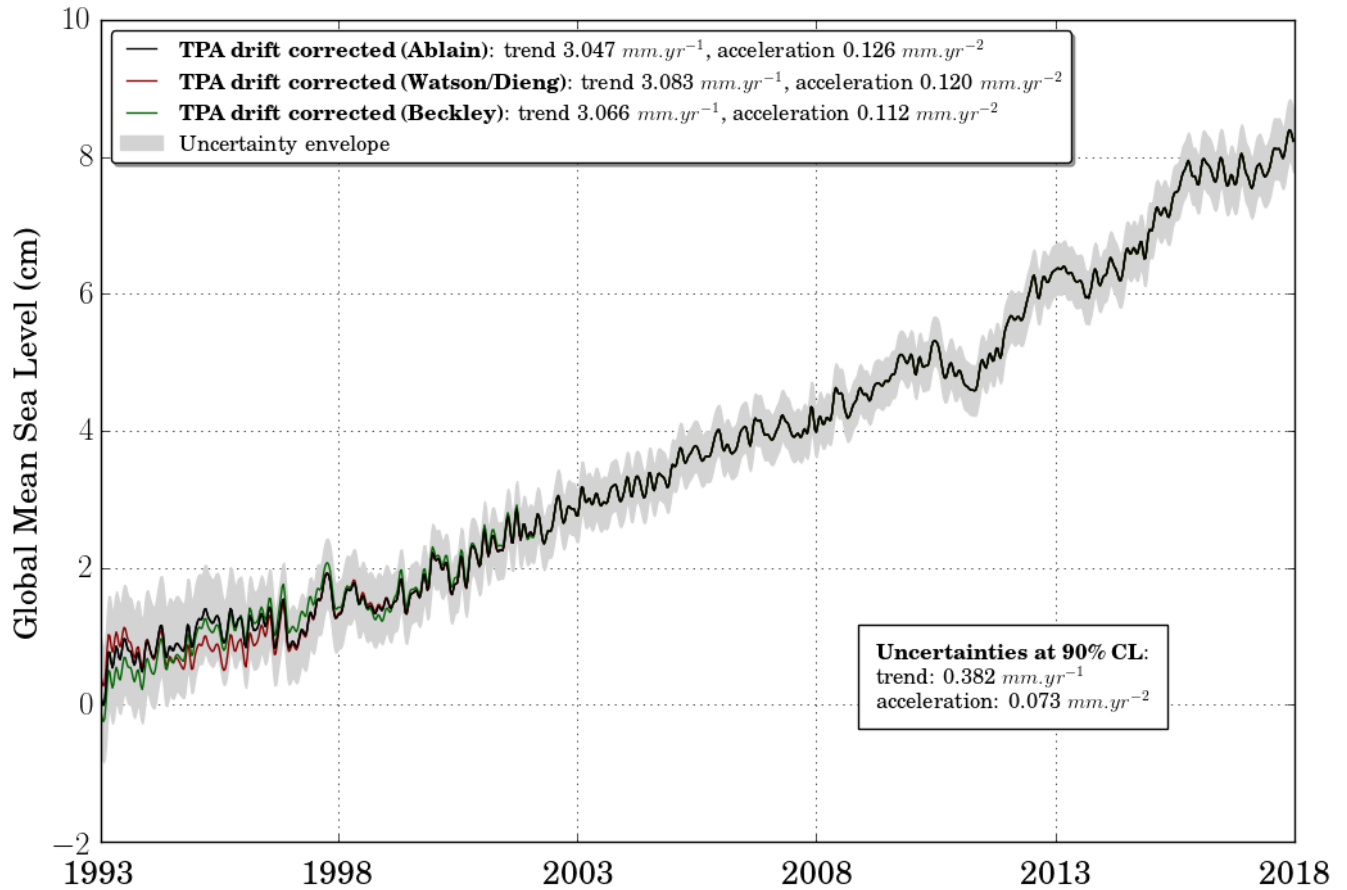


Figure 14: Evolution of the AVISO GMSL with different TOPEX-A corrections. On the black, red and green curves, the TOPEX-A drift correction is applied respectively based on (Ablain, 2017), (Watson et al., 2015), (Dieng et al., 2017) and (Beckley et al., 2017). The uncertainty envelope, as well as trend and acceleration uncertainties are given at 90% confidence level (i.e. 1.65σ). Seasonal (annual and semi-annual) signals removed and 6-month smoothing applied; GIA correction also applied.

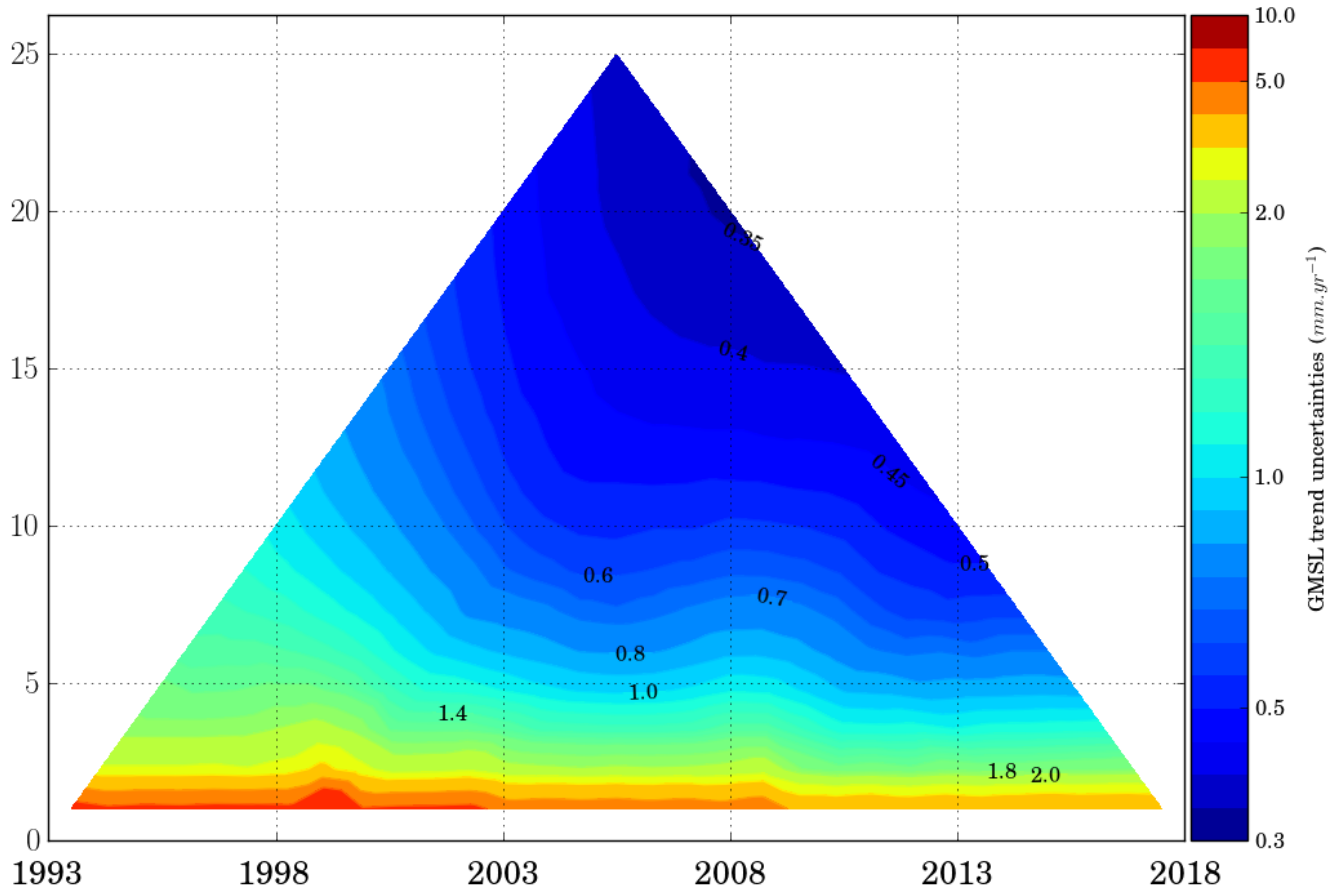


Figure 15: GMSTL trend uncertainties (mm/yr) estimated for all altimeter periods within the 25-years period (January 1993 to December 2017). The confidence level is 90 % (i.e. 1.65σ). Each colored pixel represents respectively the half-size of the 90% confidence range in GMSTL trend. Values are given in mm/yr. The vertical axis indicates the length of the period (ranging from 1 to 25 years) considered in the computation of the trend while the horizontal axis indicates the center date of the period (for example 2000 for the 20-year period 1990-2009).

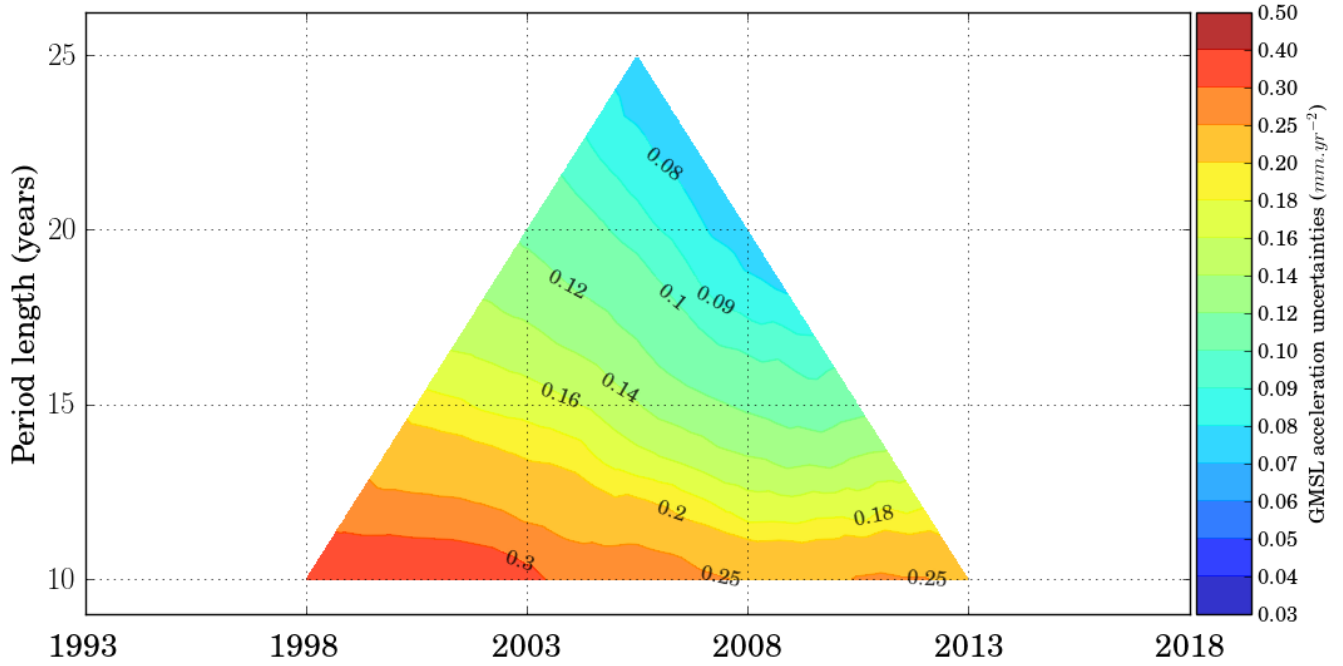


Figure 16: GMSL acceleration uncertainties (mm/yr²) estimated for all the altimeter periods within the 25-years period (January 1993 to December 2017). The confidence level is 90 % (i.e. 1.65σ). Each colored pixel represents respectively the half-size of a 90% confidence range in GMSL acceleration. Values are given in mm/yr². The vertical axis indicates the length of the period (ranging from 1 to 25 years) considered in the computation of the acceleration while the horizontal axis indicates the center date of the period (for example 2000 for the 20-year period 1990-2009).

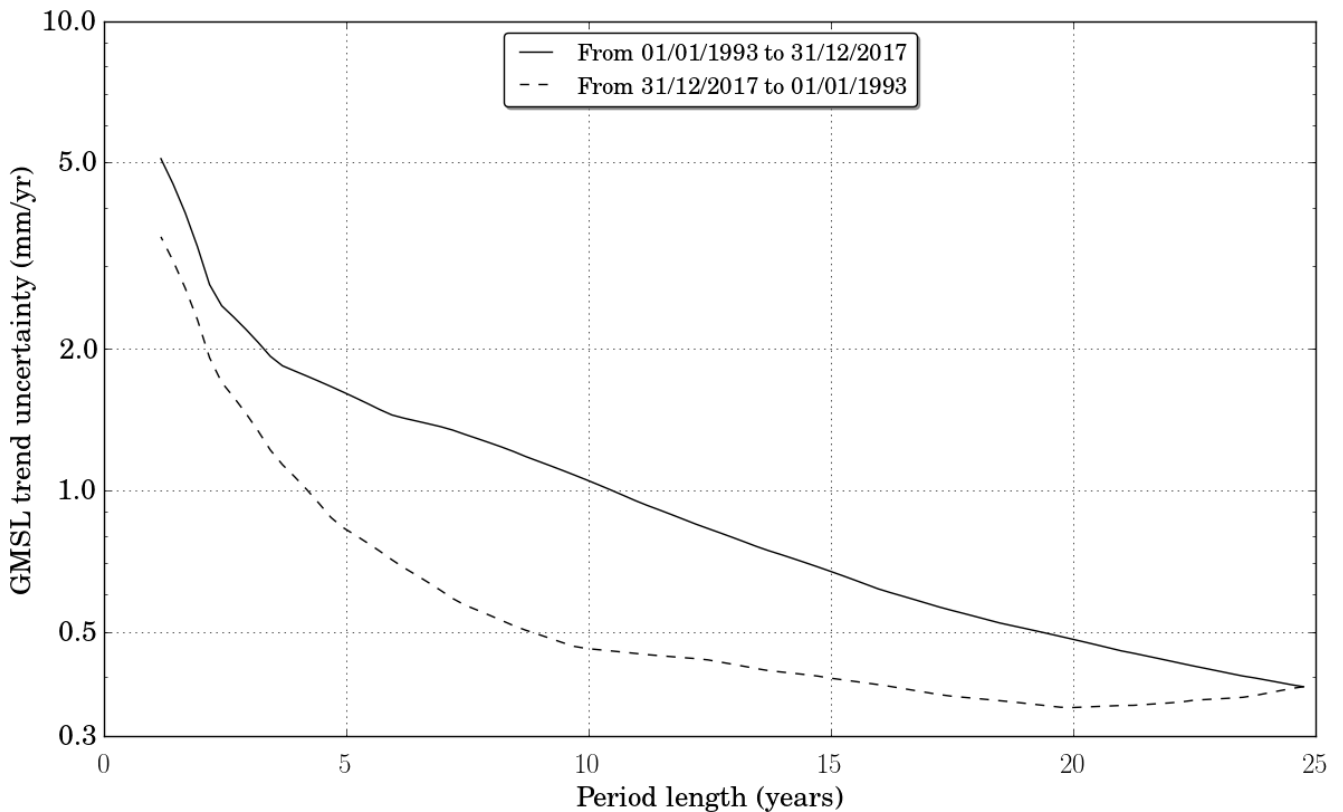




Figure 17: Evolution of GMSL trend uncertainties (within a 90% confidence level, i.e. 1.65σ) versus the altimeter period length from January 1993 to December 2017 on plain curve and from December 2017 to January 1993 on the dashed curve.

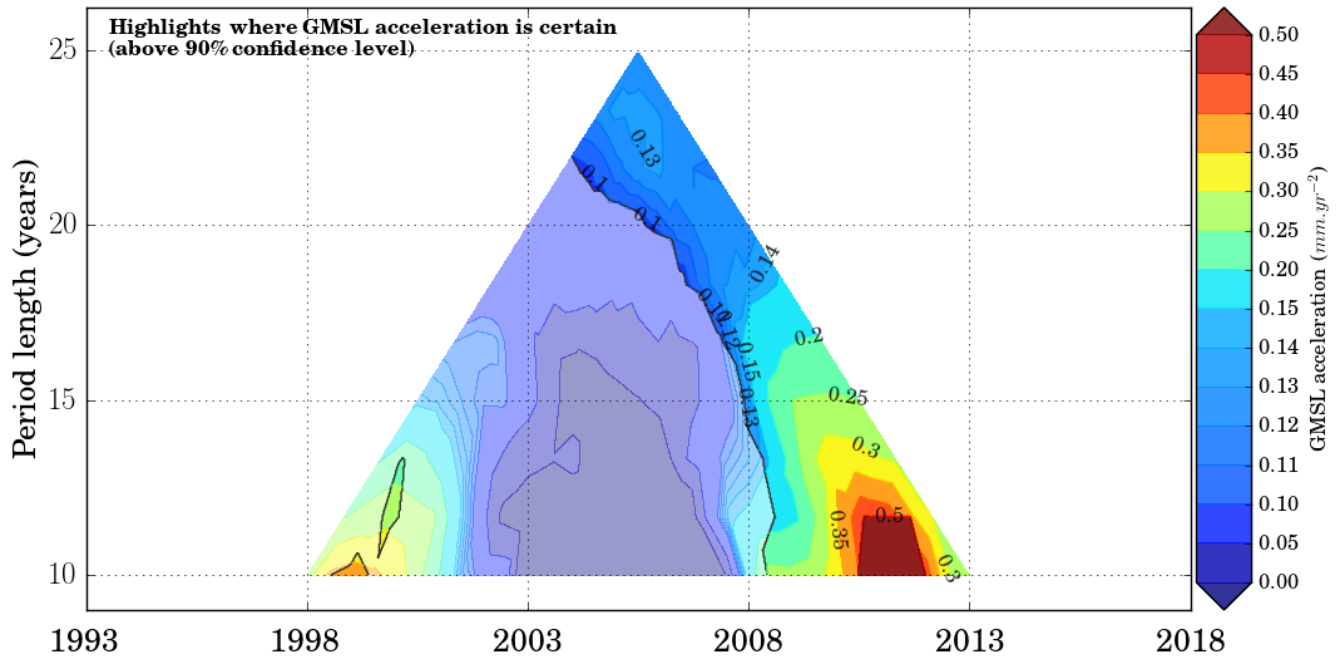


Figure 18: GMSL acceleration using the AVISO GMSL timeseries corrected for the TOPEX-A drift using the correction proposed by Ablain et al. (2018): acceleration in shaded areas is not significant (i.e. lower than acceleration uncertainties at 90% confidence level). The length of the window (in years) is represented on the vertical axis and the central date of the window used (in years) is represented on the horizontal axis.

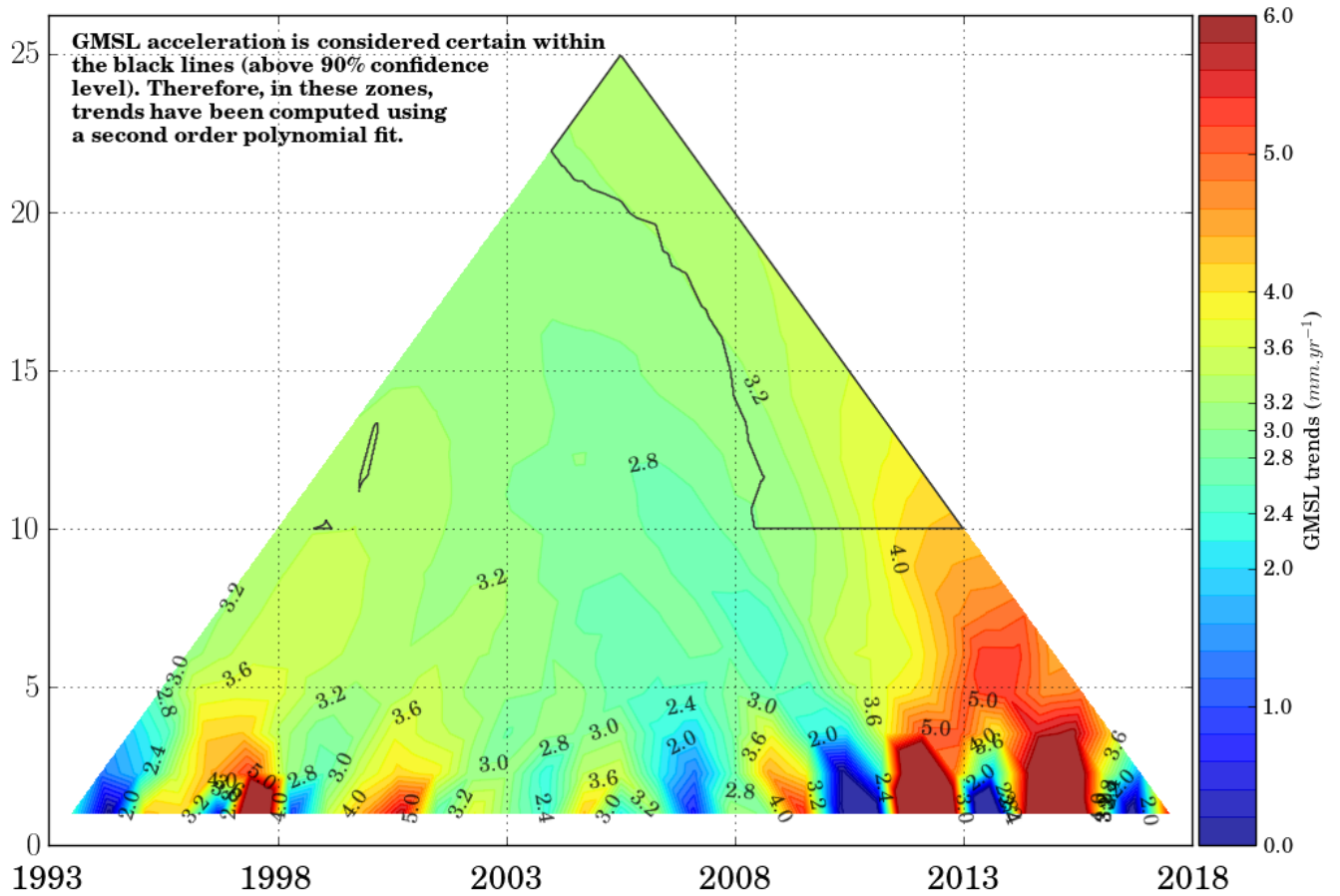


Figure 19: GMSL trends using the AVISO GMSL timeseries corrected for the TOPEX-A drift using the correction proposed by (Ablain et al., 2017). Where accelerations can be considered significant (above 90%CL, within the black lines), a second order polynomial fit has been used (see text). The length of the window (in years) is represented on the vertical axis and the central date of the window used (in years) is represented on the horizontal axis.



Source of errors	Error category	Uncertainty level (at 1 σ)	References
High frequency errors: altimeter noise, geophysical corrections, orbits ...	Correlated errors ($\lambda = 2$ months)	$\sigma = 1.7$ mm for TOPEX period $\sigma = 1.5$ mm for Jason-1 period. $\sigma = 1.2$ mm for Jason-2/3 period.	Calculation explained in this paper
Medium frequency errors: geophysical corrections, orbits ..	Correlated errors ($\lambda = 1$ year)	$\sigma = 1.3$ mm for TOPEX period $\sigma = 1.2$ mm for Jason-1 period. $\sigma = 1$ mm for Jason-2/3 period.	Calculation explained in this paper
Large frequency errors: wet troposphere correction	Correlated errors ($\lambda = 5$ years)	$\sigma = 1.1$ mm over all the period (\Leftrightarrow to 0.2 mm/yr for 5 years)	(Legeais et al., 2014; Thao et al., 2014)
Large frequency errors: orbits (Gravity fields)	Correlated errors ($\lambda = 10$ years)	$\sigma = 1.12$ mm over TOPEX period (no GRACE data) $\sigma = 0.5$ mm over Jason period (\Leftrightarrow to 0.05 mm/yr for 10 years)	(Couhert et al., 2015; Rudenko et al., 2017)
Altimeter instabilities on TOPEX-A and TOPEX-B	Drift error	$\delta = 0.7$ mm/yr on TOPEX-A period $\delta = 0.1$ mm/yr on TOPEX-B period	(Ablain, 2017; Beckley et al., 2017; Watson et al., 2015)
Long-term drift errors: orbit (ITRF) and GIA	Drift error	$\delta = 0.12$ mm/yr over 1993-2017	(Couhert et al., 2015; Spada, 2017)
GMSL bias errors to link altimetry missions together	Bias errors	$\Delta = 2$ mm for TP-A/TP-B $\Delta = 0.5$ mm for TP-B/J1, J1/J2, J2/J3.	(Zawadzki et al., 2018)

Table 1: Altimetry GMSL error budget given at 1-sigma